Electron Acceleration (and Magnetic Field) in AGN Jets

Lukasz Stawarz

KIPAC/SLAC, Stanford University

The Central Engine

Rotating black hole embedded in an external magnetic field (supported by an accretion disk) acquires a quadrupole distribution of the electric charges with the corresponding poloidal electric field (Wald 74). Thus, power can be extracted by allowing currents to flow between the equator and poles of a spinning black hole above the event horizon.

Blandford & Znajek 77 discussed how, with a force-free magnetosphere added to such a rotating black hole, electromagnetic currents are driven, and how the energy is released (in a form of magnetized jets) in the expense of the black hole rotational energy ("reducible mass"). For the conserved magnetic flux and maximally rotating black hole, the maximum energy and power that can be extracted in this way are:

$$E_{tot} \sim 0.3\ M\ c^2 \sim 10^{63}\ (M/10^9 M_\odot)\ [erg]$$
$$P_{max} \sim c\ B^2\ r_g^{\,2} / 4\pi \sim 10^{46}\ (M/10^9 M_\odot)\ [erg/s]$$

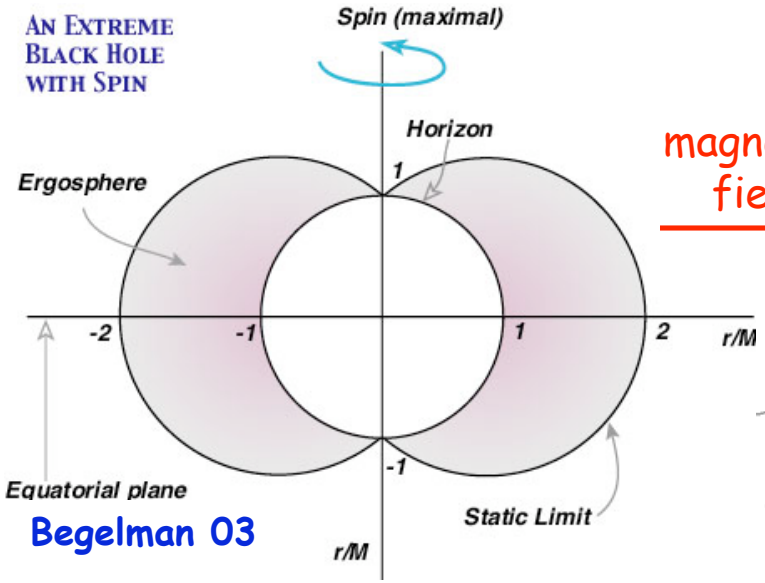

Begelman 03

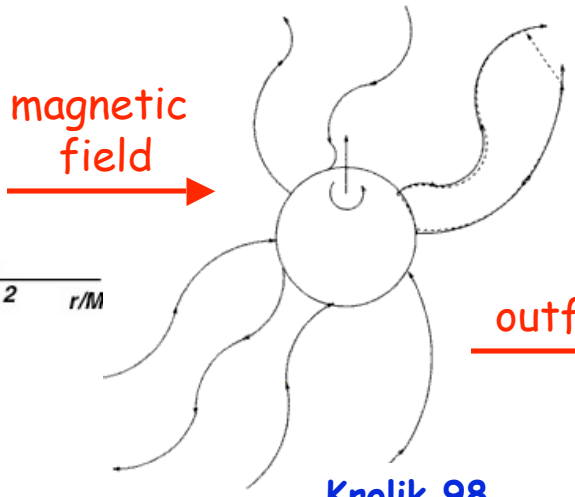

Krolik 98

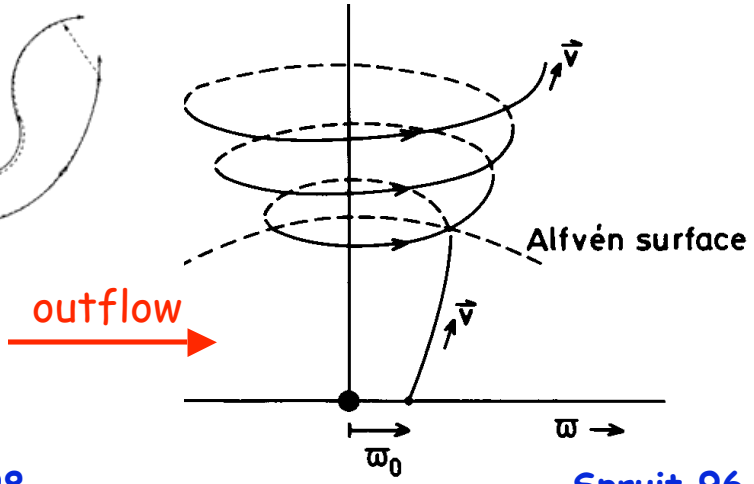

Spruit 96

Magnetized Jets

The most recent GR MHD simulations confirm that relativistic jets are indeed launched via the Blandford & Znajek process. Such jets are dominated by the toroidal magnetic field, and are characterized by the gradual collimation and acceleration up to at least ~10^3 r_g . Beyond this distance, the current-driven (pinch and kink) instabilities develop within an outflow, which may lead to formation of shocks. Such shocks convert magnetic energy to the internal energy of the jet plasma, accelerating jet particles to ultrarelativistic energies.

Is this conversion of Poynting flux to matter-dominated outflow related to the blazar phenomenon? Where does it happen (if it does)?

Koide+ 02

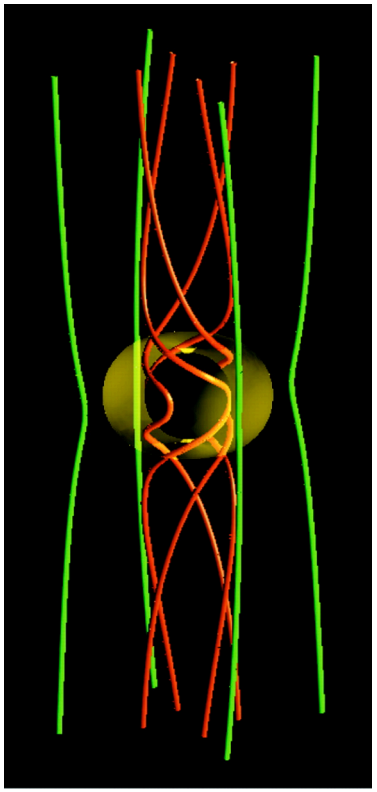

Hawley & Krolik 06

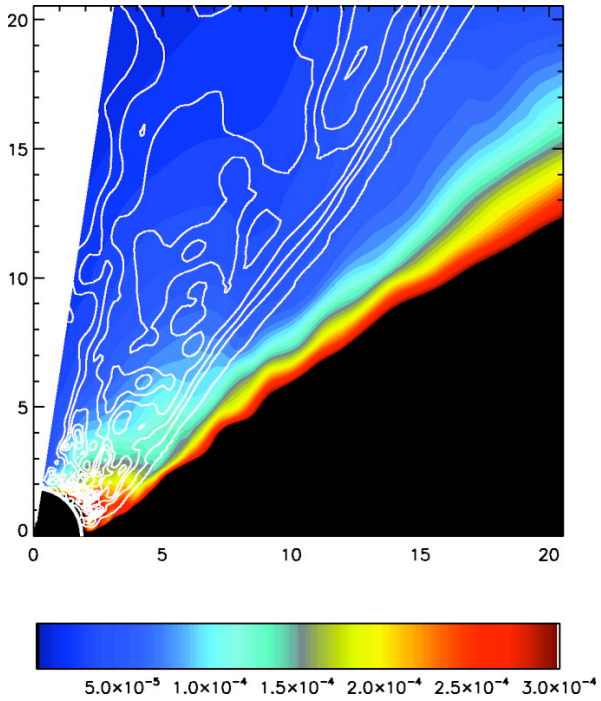

Mizuno+ 07

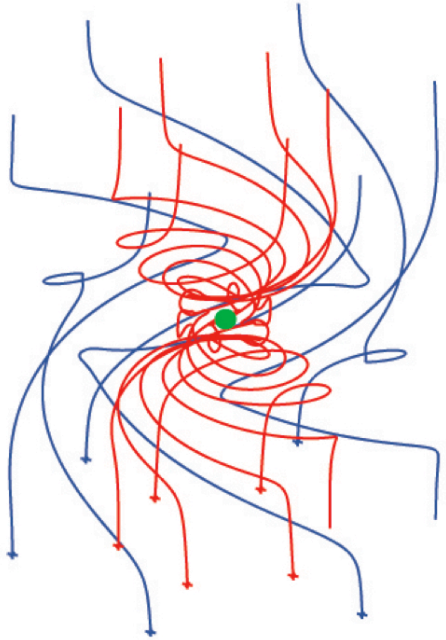

McKinney 06

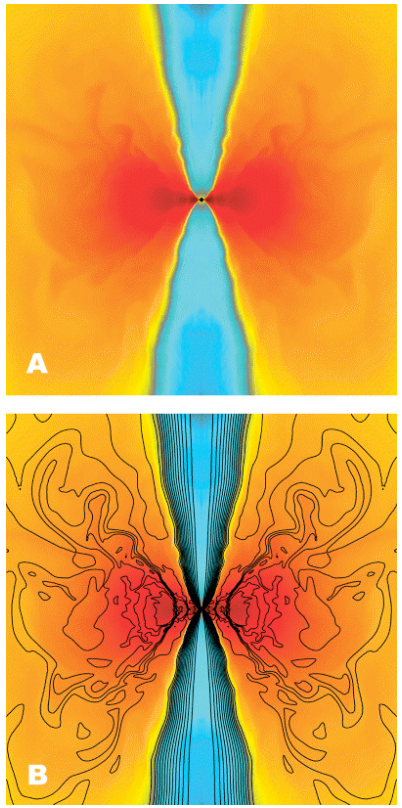

Blazar Phenomenon

Leptonic Models **(Maraschi+ 91, Dermer & Schlickeiser 93, Sikora+ 94, Levinson & Blandford 95, Marscher & Travis 96)**: Low- and high energy components due to, respectively, synchrotron and inverse-Compton emission of ultrarelativistic electrons accelerated directly within the outflow.

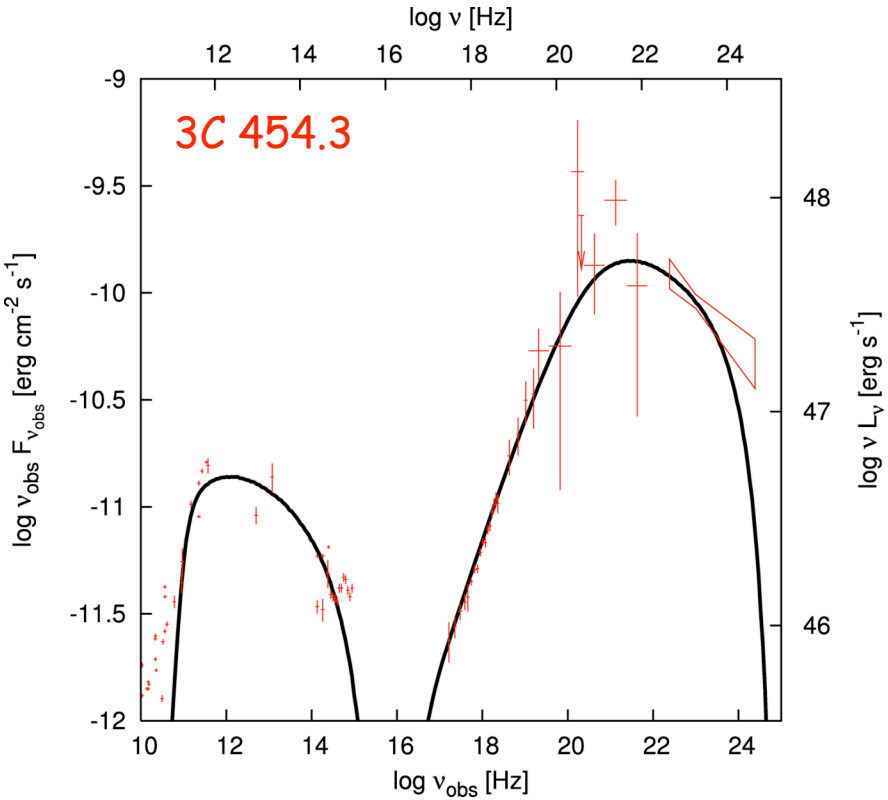

Hadronic Models **(Mannheim & Biermann 92, Mannheim 93 Aharonian 00)**: High-energy emission of relativistic protons directly accelerated within the outflow (photomezon production, synchrotron proton emission); low-energy component due to synchrotron emission of primary or secondary electrons.

In the framework of a "standard" leptonic blazar scenario, one-zone homogeneous emission zone is assumed. This simple model is relatively successful in explaining several properties of blazar sources established so far. If this is the case indeed, the question to be asked is why there is only one, well defined and very compact region of the enhanced energy dissipation within the outflow, rather than a superposition of different emission zones)? But if the homogeneous one-zone approximation is correct, and if the blazar region is located close to the center, then one should expect strong magnetic field within the blazar emission zone, and hence no standard shock acceleration.

FSRQs

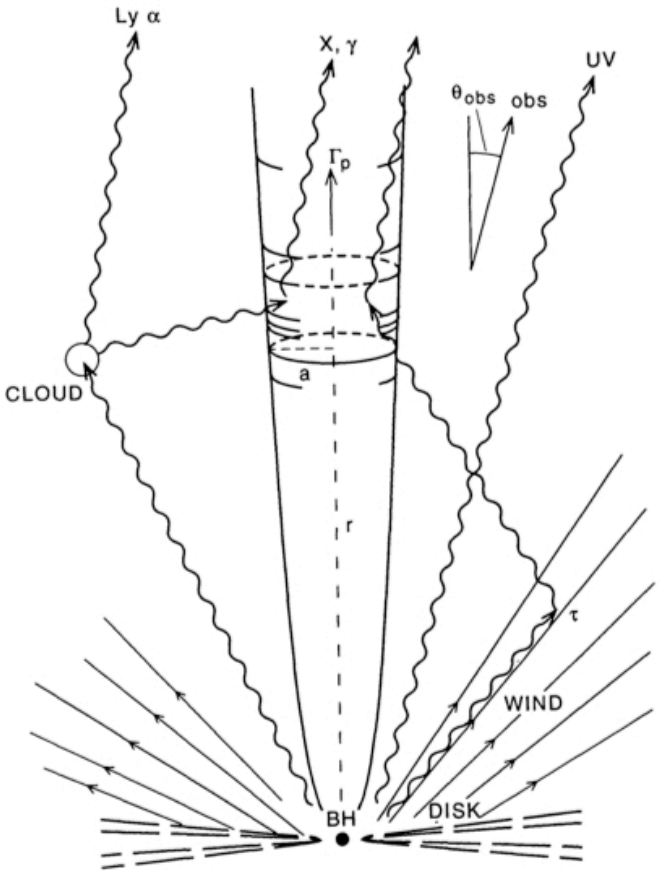

Modeling of the broad-band blazar emission (and its variability) in a framework of the leptonic scenario (see **Sikora+ 09** and references therein) allows to put some constraints on the physical parameters of the blazar emission region. In particular, such modeling indicate that:

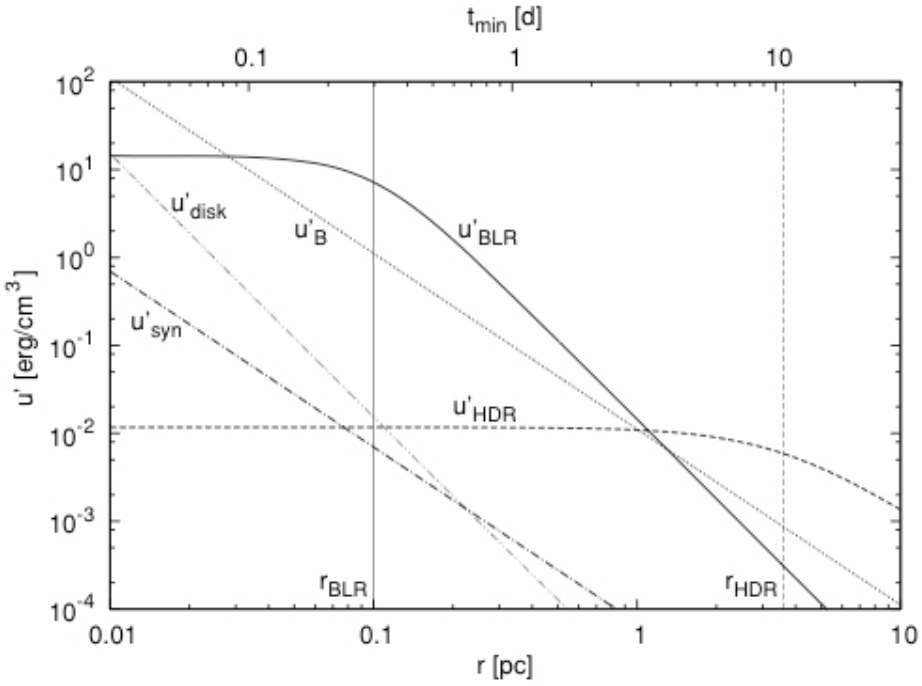

1) Emission regions are compact, R ~ 10^{16} - 10^{17} cm .
2) Implied highly relativistic bulk velocities of the emitting regions, Γ ~ 10-30 , are in agreement with the ones inferred from the observed superluminal motions of VLBI jets on pc scales.
3) Energy density of magnetic field is at most equal to the energy density of radiating ultrarelativistic electrons, $U_B \leq U_{e,rel}$.
4) The implied magnetic intensity B ~ 0.1-1 *G* is consistent with the one inferred from the SSA features in compact radio cores.
5) Distance of the emission region from the center is not well constrained, typically r ~ 10^{17} - 10^{19} cm

Jet Power

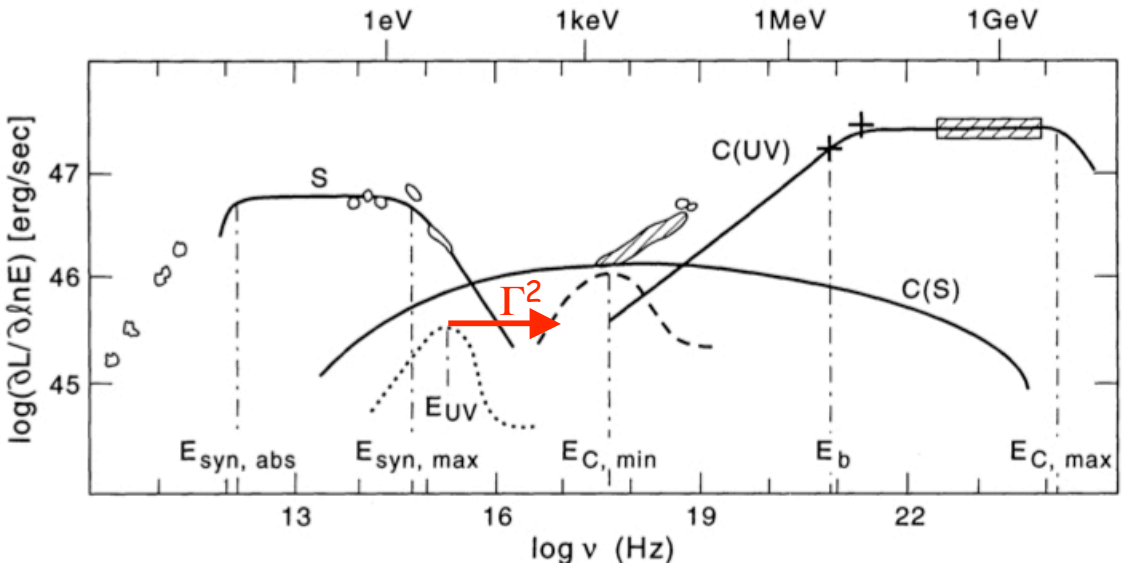

In addition, the power carried by ultrarelativistic electrons cannot account for the total radiated power of blazars, or for the kinetic power of quasar jets deposited far away from the active nucleus (e.g., **Celotti & Ghisellini 08**). So either

(1) MF is dominating dynamically, while blazar emission is produced in small jet sub-volumes with MF intensity lower than average (?), or

(2) jets on blazar scales are dynamically dominated by protons and/or cold electrons.

However, lack of bulk-Compton features in soft-X-ray spectra of blazars (**Begelman & Sikora 87, Sikora+97, Sikora & Madejski 00, Moderski+ 04, Celotti+ 07**) indicates that

(3) cold electrons cannot carry bulk of the jet power.

➔ **indication for the dynamical role of (cold) protons**

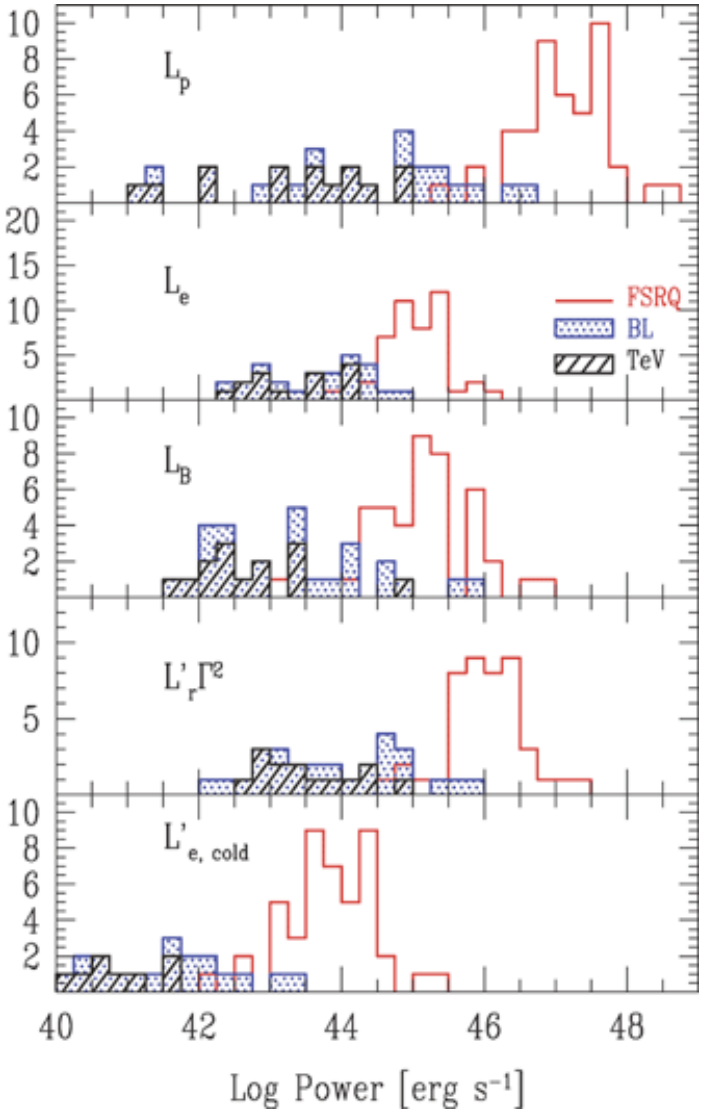

Shock Spectra of Blazar Jets

Energy distribution of the radiating electrons:

$$n_e(\gamma) \propto$$

$$\gamma^{-1.35} \text{ for } \gamma < \gamma_{br} \sim 100$$
$$\gamma^{-3.35} \text{ for } \gamma > \gamma_{br} \sim 100$$

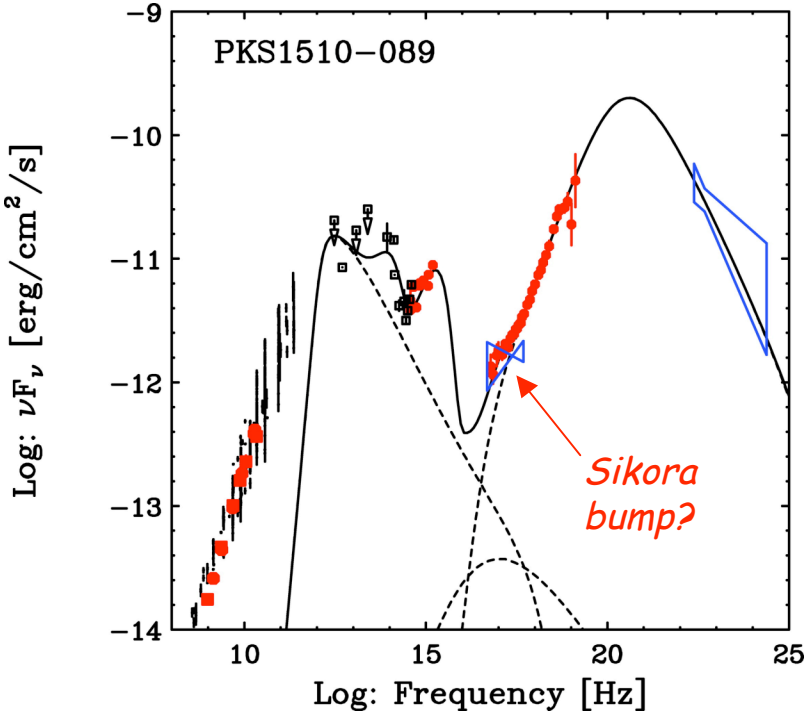

Kataoka+ 08: parameters of blazar PKS 1510-089

$\Gamma \sim 20$,
$r \sim 1$ pc , $R \sim 10^{16}$ cm ,
$N_e/N_p \sim 10$, $B \sim 0.6$ G ,
$L_p \sim 2 \times 10^{46}$ erg/s ,
$L_e \sim 0.1 \times 10^{46}$ erg/s ,
$L_B \sim 0.6 \times 10^{46}$ erg/s

The implied physical parameters of the blazar emission zone, as well as the spectral energy distribution of the emitting ultrarelativistic electrons being consistent with the shock acceleration scenario **(though not the "standard" diffusive shock acceleration model!)** suggest that the extragalactic jets are matter (proton) dominated already at sub-pc scales

Shock Spectra of Blazar Jets

Energy distribution of the radiating electrons:

$$n_e(\gamma) \propto$$

$\gamma^{-1.35}$ for $\gamma < \gamma_{br} \sim 100$

$\gamma^{-3.35}$ for $\gamma > \gamma_{br} \sim 100$

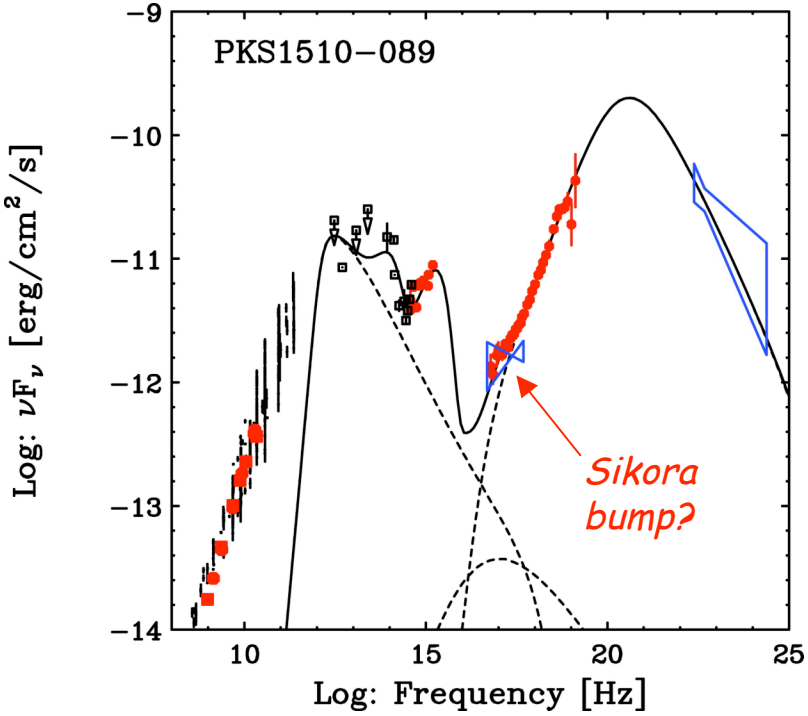

The implied physical parameters of the blazar emission zone, as well as the spectral energy distribution of the emitting ultrarelativistic electrons being consistent with the shock acceleration scenario **(though not the "standard" diffusive shock acceleration model)** suggest that the extragalactic jets are matter (proton) dominated already at sub-pc scales (self-consistent scenario!)

Kataoka+ 08: parameters of blazar PKS 1510-089

$\Gamma \sim 20$,
$r \sim 1$ pc , $R \sim 10^{16}$ cm ,
$N_e/N_p \sim 10$, $B \sim 0.6$ G ,
$L_p \sim 2 \times 10^{46}$ erg/s ,
$L_e \sim 0.1 \times 10^{46}$ erg/s ,
$L_B \sim 0.6 \times 10^{46}$ erg/s

Low-Energy Electron Spectra

Table 1
Luminous Blazar Sources with the Hardest Recorded X-ray Spectra

Name (1)	z (2)	α_x (3)	α_γ^E (4)	α_γ^F (5)	Reference (6)
S5 0212+73	2.367	0.32 ± 0.19	...	...	Sambruna et al. (2007)
PKS 0229+13	2.059	0.39 ± 0.09	...	...	Marshall et al. (2005)
PKS 0413-21	0.808	0.39 ± 0.12	...	...	Marshall et al. (2005)
PKS 0528+134	2.060	0.12 ± 0.26	1.46 ± 0.04	1.54 ± 0.09	Donato et al. (2005)
PKS 0537-286	3.104	0.27 ± 0.02	1.47 ± 0.60	...	Reeves et al. (2001)
PKS 0745+241	0.409	0.35 ± 0.12	...	...	Marshall et al. (2005)
SWIFT J0746.3+2548	2.979	0.17 ± 0.01	...	...	Watanabe et al. (2009)
PKS 0805-07	1.837	0.20 ± 0.20	$1.34 \pm 0.29(?)$	...	Giommi et al. (2007)
S5 0836+710	2.172	0.34 ± 0.04	1.62 ± 0.16	...	Donato et al. (2005)
RGB J0909+039	3.200	0.26 ± 0.12	...	...	Giommi et al. (2002)
PKS 1127-145	1.184	0.20 ± 0.03	1.70 ± 0.31	1.69 ± 0.18	Siemiginowska et al. (2008)
PKS 1424-41	1.522	0.20 ± 0.30	1.13 ± 0.21	...	Giommi et al. (2007)
GB 1428+4217	4.715	0.29 ± 0.05	...	...	Fabian et al. (1998)
PKS 1510-089	0.360	0.23 ± 0.01	1.47 ± 0.21	1.48 ± 0.05	Kataoka et al. (2008)
PKS 1830-211	2.507	0.09 ± 0.05	1.59 ± 0.13	...	De Rosa et al. (2005)
PKS 2149-306	2.345	0.38 ± 0.08	...	...	Donato et al. (2005)
PKS 2223+210	1.959	0.31 ± 0.26	...	...	Donato et al. (2005)
3C 454.3	0.859	0.34 ± 0.06	1.21 ± 0.06	1.41 ± 0.02	Donato et al. (2005)

Notes. (1) Name of a source; (2) redshift of a source, z; (3) X-ray spectral index, α_x; (4) EGRET γ-ray spectral index, α_γ^E (Hartman et al. 1999); (5) *FERMI* γ-ray spectral index, α_γ^F (Abdo et al. 2009b); and (6) references.

X-ray spectra of luminous blazars are very flat, implying that the low-energy electron spectra $s \sim 1.4 - 1.8$ are common (**Sikora+ 09**)

Relativistic p+e- Shocks

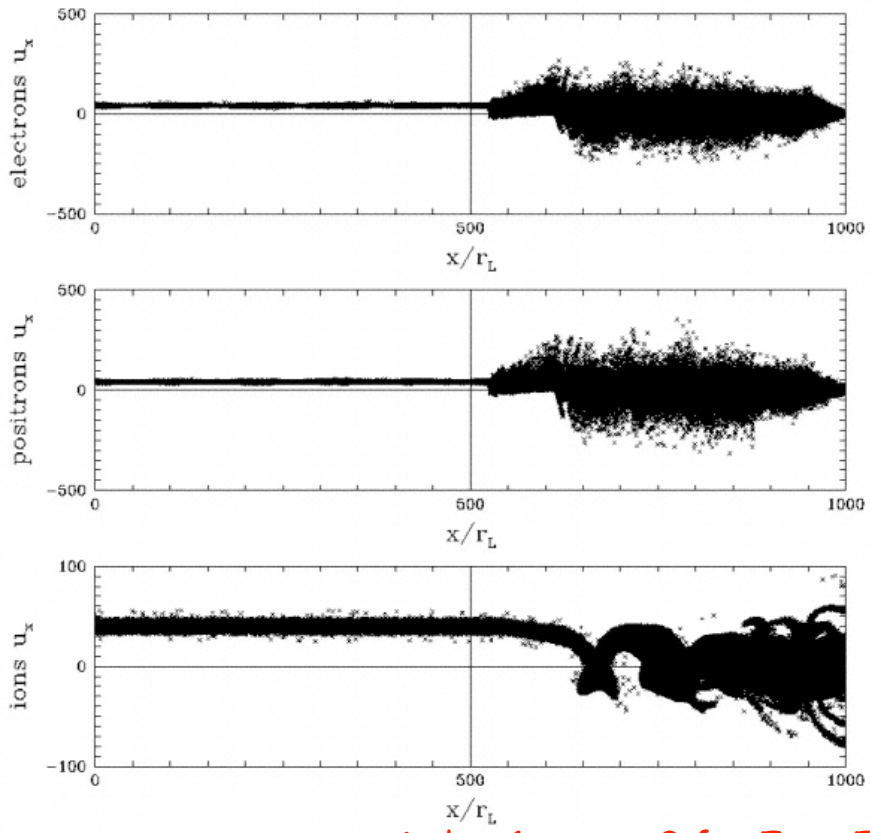

energy index **1 < s < 2** for $E_e < E_p$

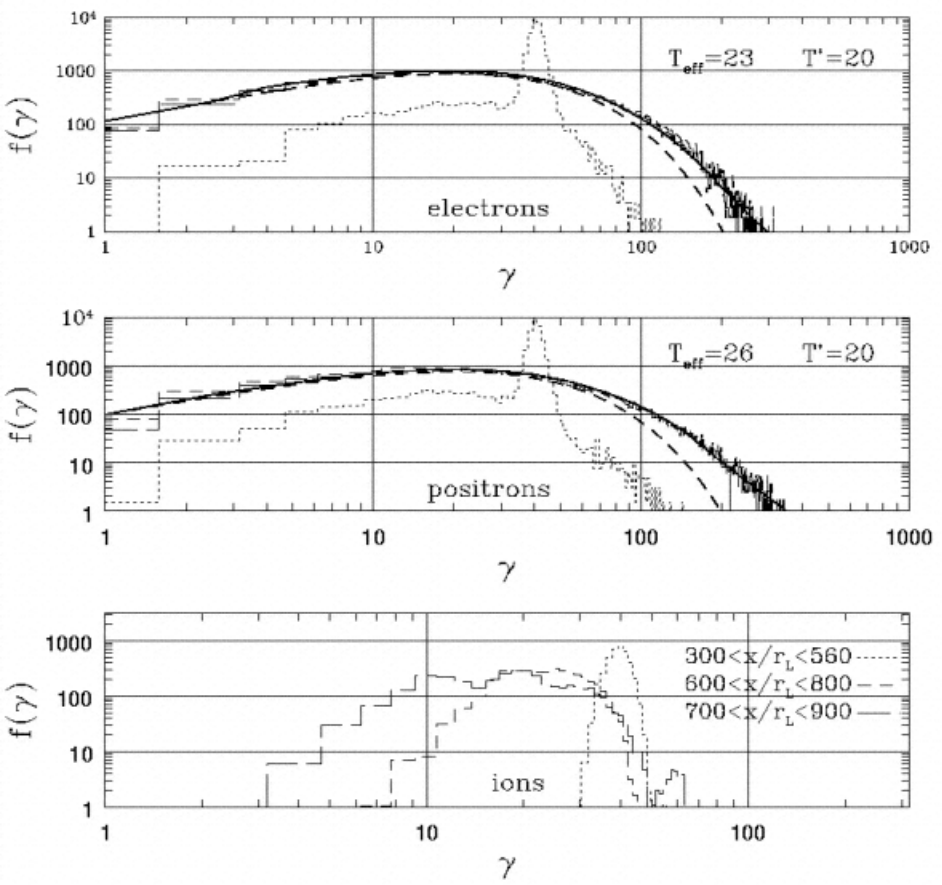

PIC simulations show that within the velocity transition region of (mildly)relativistic, proton-mediated, transverse shocks, **e+e- with gyroradii smaller than the shock thickness (~ few proton gyroradii)** can absorb electromagnetic cyclotron waves emitted at high harmonics by cold protons reflected from the shock front. The resulting e+e- spectra are consistent with a flat (1<s<2) power-law between electron energies $\gamma \sim \Gamma_{sh}$ and $\gamma \sim \Gamma_{sh}\,(m_p/m_e)$ (**Hoshino+ 92; Amato & Arons 06**).

Diffusive Shock Acceleration

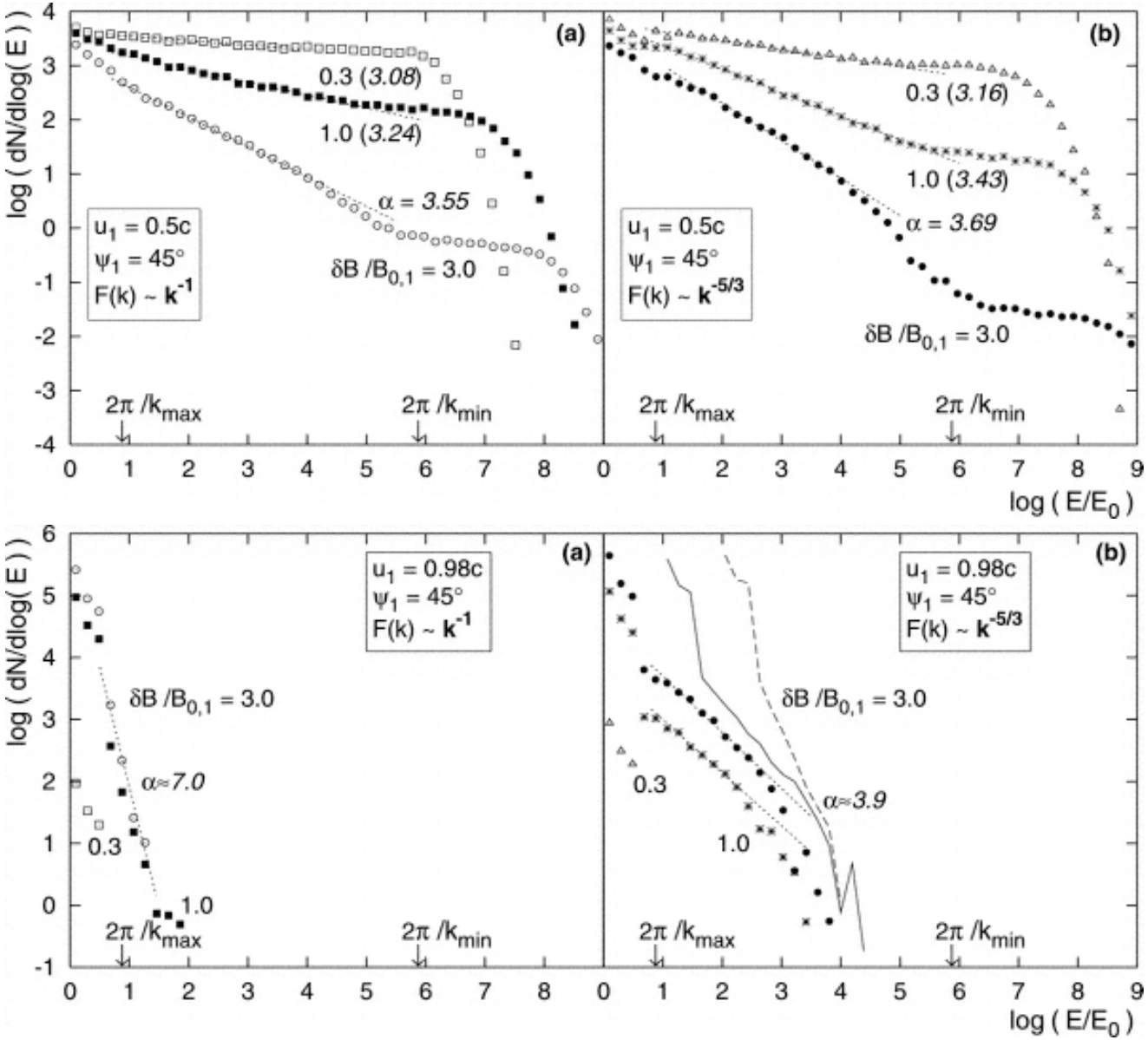

MC simulations reveal variety of particle spectra resulting from 1st-order Fermi acceleration at **relativistic** subluminal or superluminal shocks (left and right panels). Previous claims of the "universal" shock spectrum (s=2.2, first found by **Bednarz & Ostrowski 98**) were based on simulations or calculations involving unphysical / unrealistic conditions (see **Ostrowski 02, Niemiec & Ostrowski 04, 06, Lemoine+ 06, Pelletier+ 09**).

energy index **s > 2** for $E_e > E_p$

BL Lacs

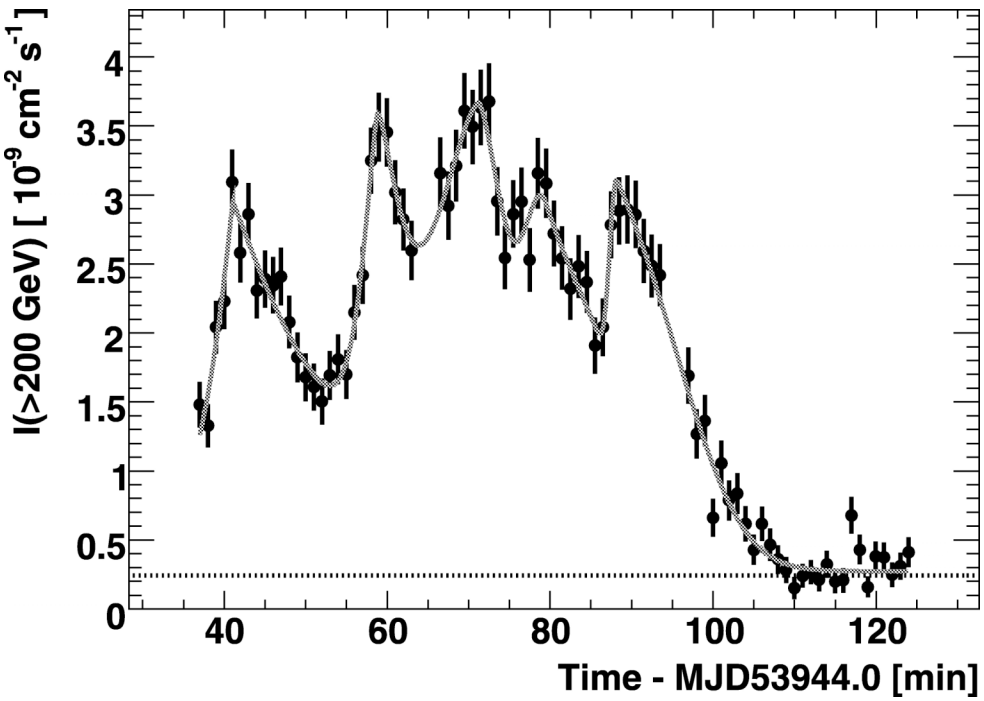

Aharonian+ 07: The shortest observed variability timescales $t_{var} < 200\ s$ imply linear sizes of the emitting region $R < c\ t_{var}\ \delta$. With the expected mass of SMBH in PKS 2155-304, $M_{BH} \sim 10^9\ M_{sun}$, this gives $R \sim (\delta/100) \times R_g$

Should we expect shocks at such small scales? (strong magnetic field!)

Low-power BL Lacs are substantially different from high-power, quasar-hosted blazars (FSRQs). They accrete at low rates, and lack intense circumnuclear photon fields. Blazar emission zone in BL Lacs seems to be located very close to the central SMBH, as indicated by a complex and rapid variability.

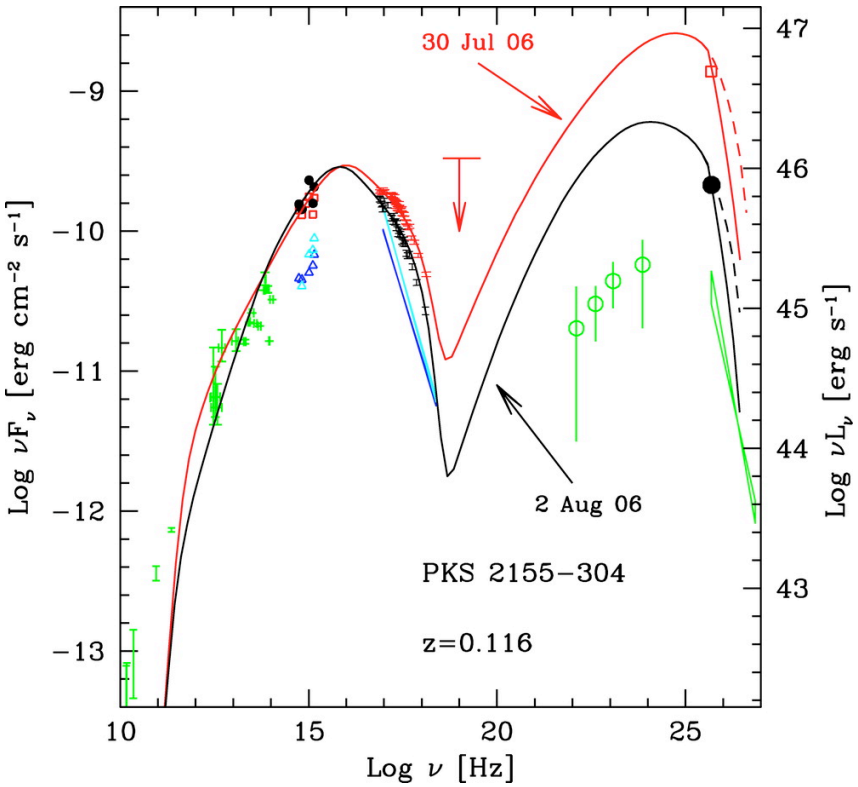

Synchrotron Spectra of BL Lacs

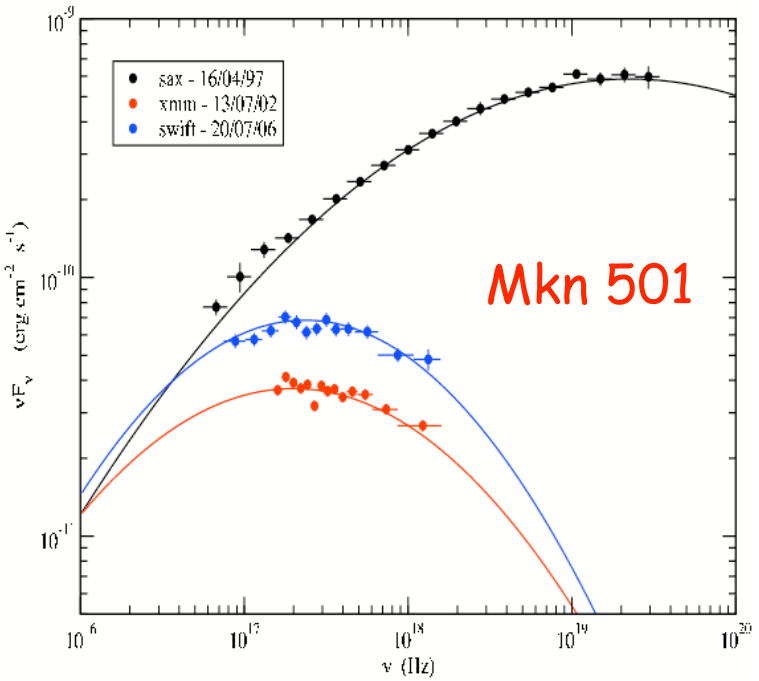

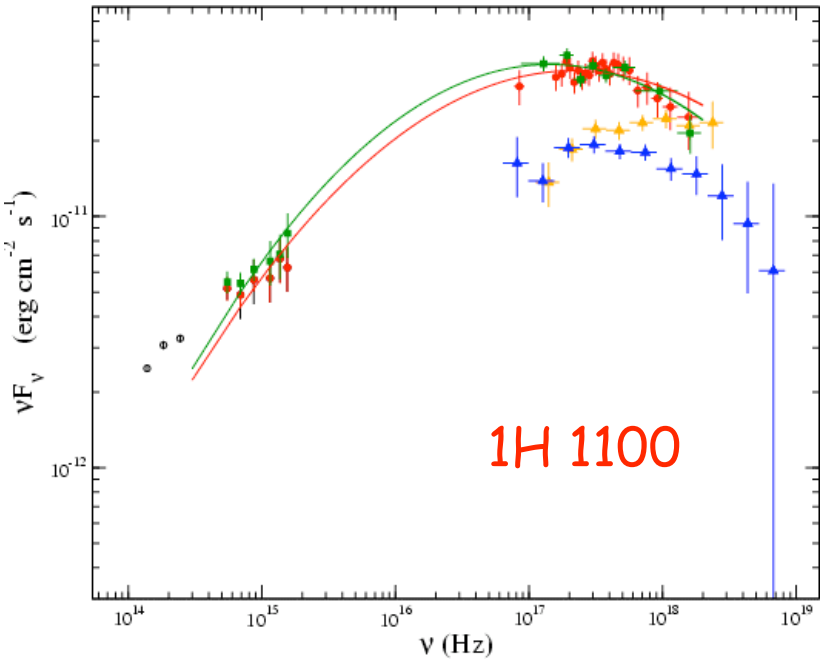

UV-X-ray spectra of BL Lacs are smoothly curved. They cannot be really fitted by "a power-law and an exponential cut-off" form, $F(E) \propto E^{-\Gamma} \exp(-E/E_{cr})$. Instead, "log-parabolic" shape represents the X-ray continua well, $F(E) \propto E^{-a + b \cdot \log(E/Ecr)}$ **(Landau+ 86, Krennrich+ 99, Giommi+ 02, Perri+ 03, Massaro+ 03, 08, Perlman+ 05, Tramacere+ 07).**

Caution: analysis of the X-ray spectra is hampered by the unknown/hardly known intrinsic absorbing column density. In the case of BL Lacs, on the other hand, such absorption is not expected to be significant. Analysis of the optical spectra are hampered by the contribution of the elliptical host.

Ultrarelativistic Maxwellian

As long as particle escape from the acceleration region is inefficient, stochastic acceleration of ultrarelativistic particles undergoing radiative cooling $t_{rad} \propto E^x$ tends to establish modified ultrarelativistic Maxwellian spectrum

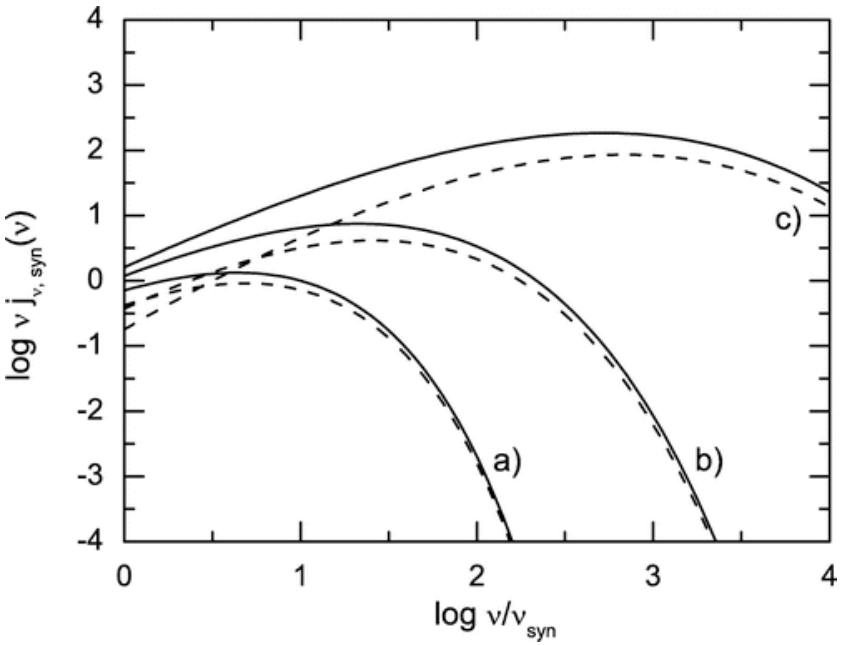

$$n(E) \propto E^2 \times \exp[- (1/a) (E/E_{eq})^a]$$

where $W(k) \propto k^{-q}$ is the energy spectrum of the turbulence, $a = 2-q-x$, and E_{eq} is the maximum particle energy defined by the balance between the acceleration and losses timescales, $t_{acc}(E_{eq}) = t_{rad}(E_{eq})$

(Schlickeiser 84, Henri & Pelletier 91, Park & Petrosian 95, Sauge & Henri 04, Katarzynski+ 06, Giebels+ 07, Boutellier+ 08, LS & Petrosian 08).

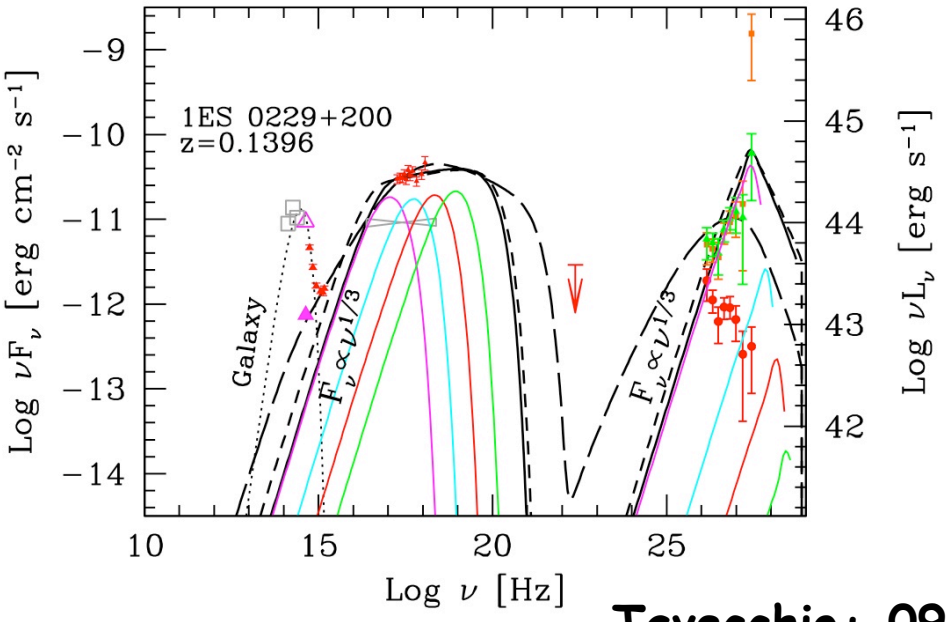

Tavecchio+ 09

Where Is the Blazar Zone?

Kovalev+ 07

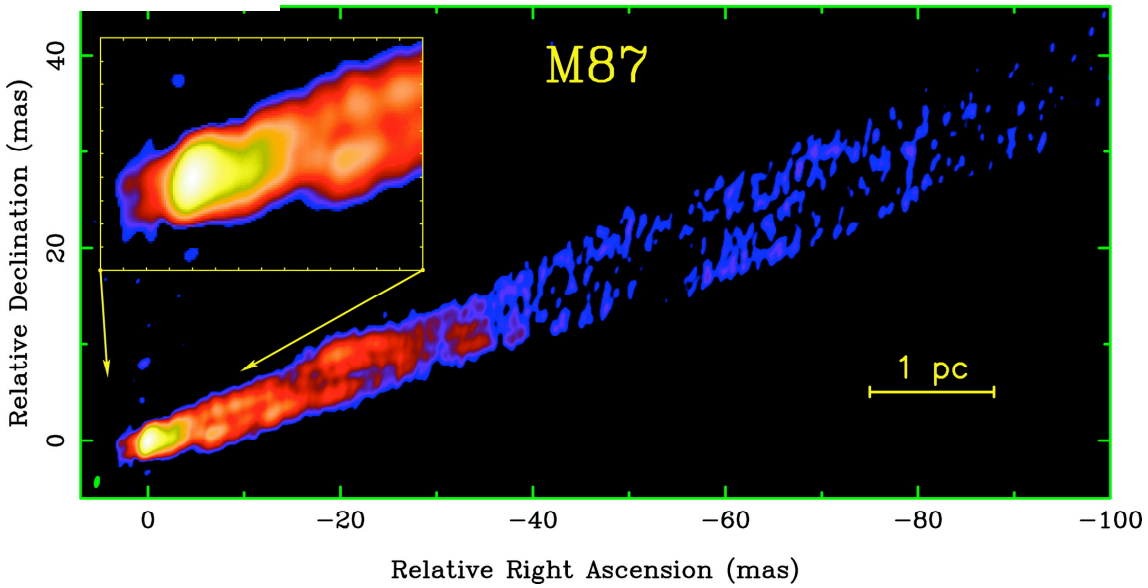

In M87, from 100 r_g up to 10^6 r_g we see almost featureless, limb-brightened, slowly collimating outflow, and… nothing else (**Junor+ 99, Dodson+ 06, Ly+ 07, Kovalev+ 07**).

Is it a Poynting-flux, or a matter-dominated outflow? Where is the the blazar emission zone?

Abdo+ 09

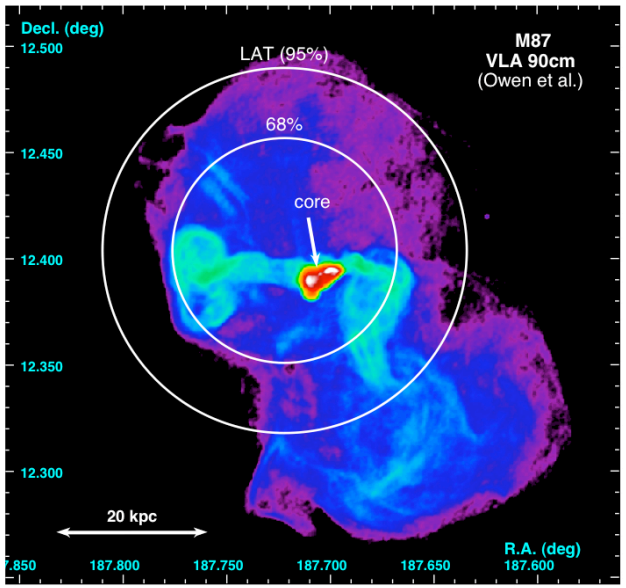

Acciari+ 09

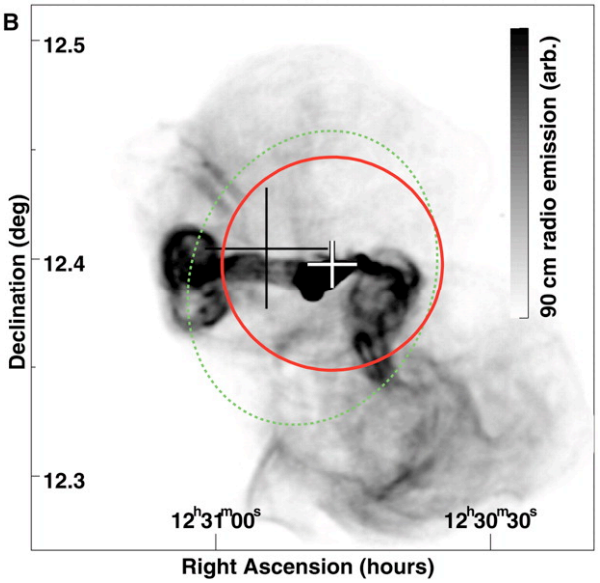

M87 has been detected at TeV photon energies by all IACTs (HEGRA, HESS, Magic, VERITAS; **Aharonian+ 03, 06, Acciari+ 08, 09, Albert+ 08**), as well by Fermi/LAT at GeV photon energies (**Abdo+ 09**).

Reconfinement Shock

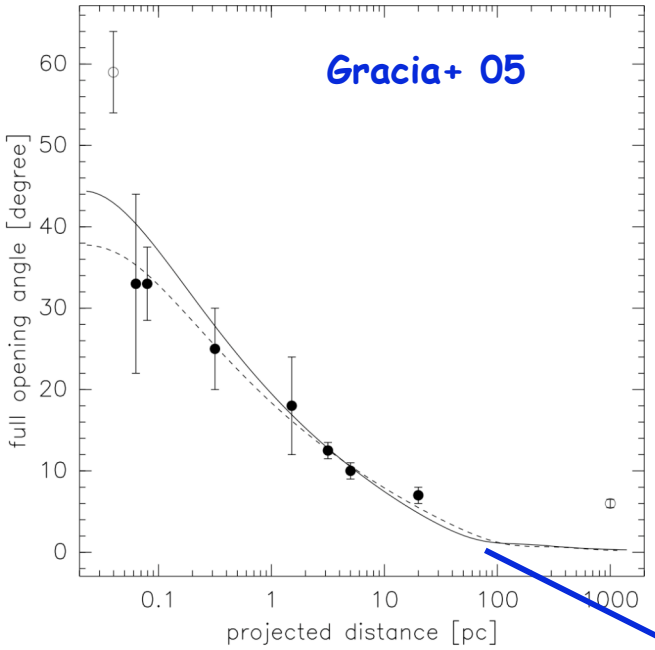

MHD models provide very good fits to the observed gradual change of the jet opening angle along M87 jet up to 100 pc distances from the center. In addition, radio flux profiles (both along and across the jet) may be explained (**Gracia+ 05, 08, Zakamska+ 08**).

Around 100pc (~10^6 r_g) from the M87 nucleus, compact (unresolved), stationary, and variable feature HST-1 is observed in radio, optical, and X-rays (**Biretta+ 99, Harris+ 03, 06, 09, Perlman+ 03, Cheung+ 07**). Downstream of this knot, superluminal blobs have been detected.

Cheung+ 07

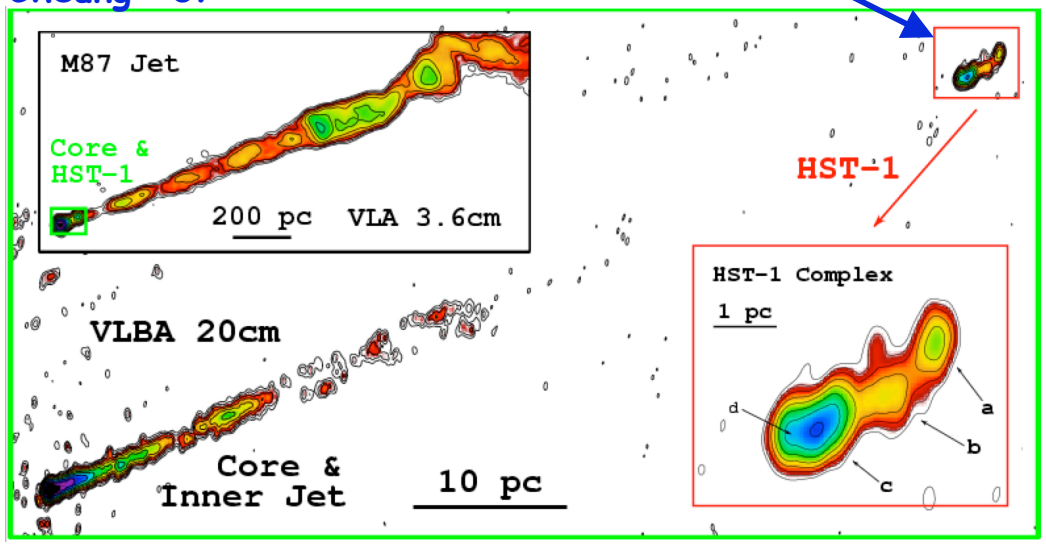

HST-1 knot may be understood as a reconfinement nozzle formed within the outflow collimated by the external gaseous medium (**LS+ 06**).

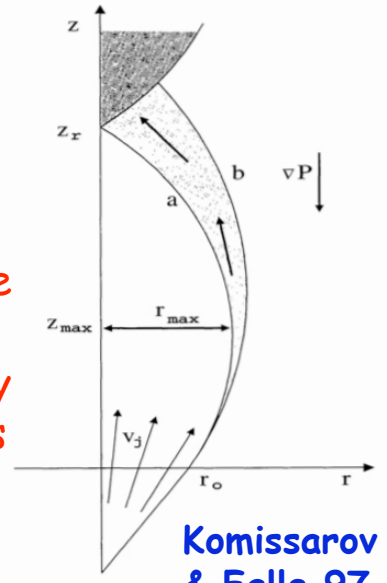

Komissarov & Falle 97

Gamma-rays From Far Away?...

In 2003/07, the TeV outburst of M87 coincided with the radio-to-X-ray flare of HST-1 knot. Around the maximum of the flare, stationary HST-1 knot ejected super-luminal radio blobs ($v_{app} \leq 4$ c).

TeV emission: day variability

Radio, optical, X-ray emission of HST-1 knot: weeks/month variability

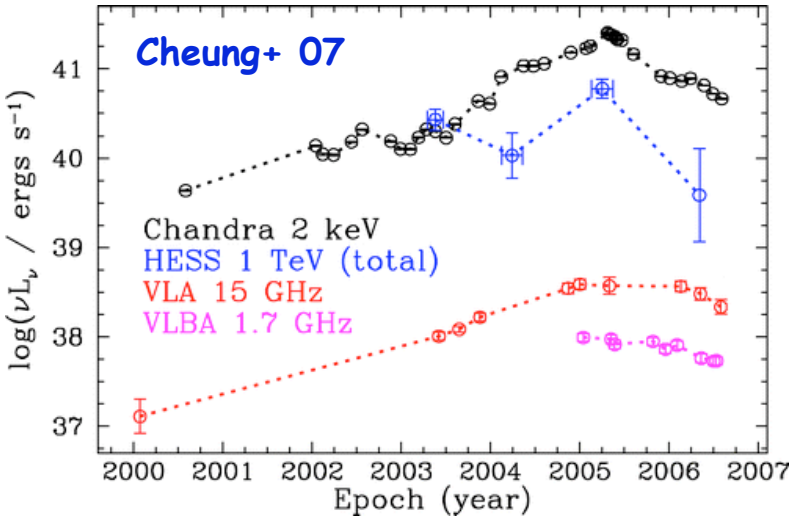

Aharonian+ 07

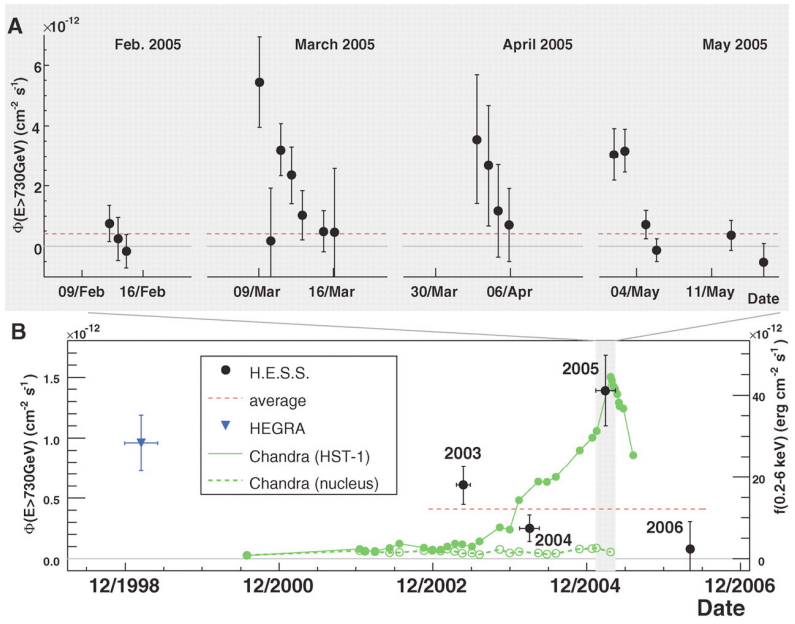

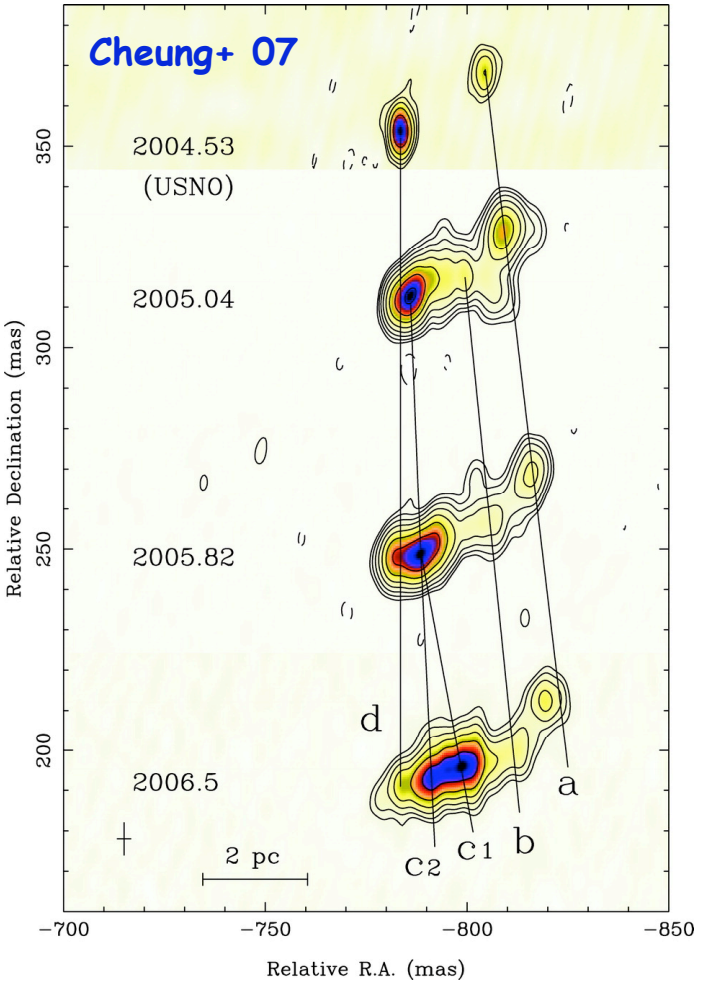

$r \sim 100$ pc

$R_{HST} < 0.2$ pc

$R_X < 0.02\ \delta$ pc

$R_{TeV} < 0.002\ \delta$ pc

… Or From the Center?

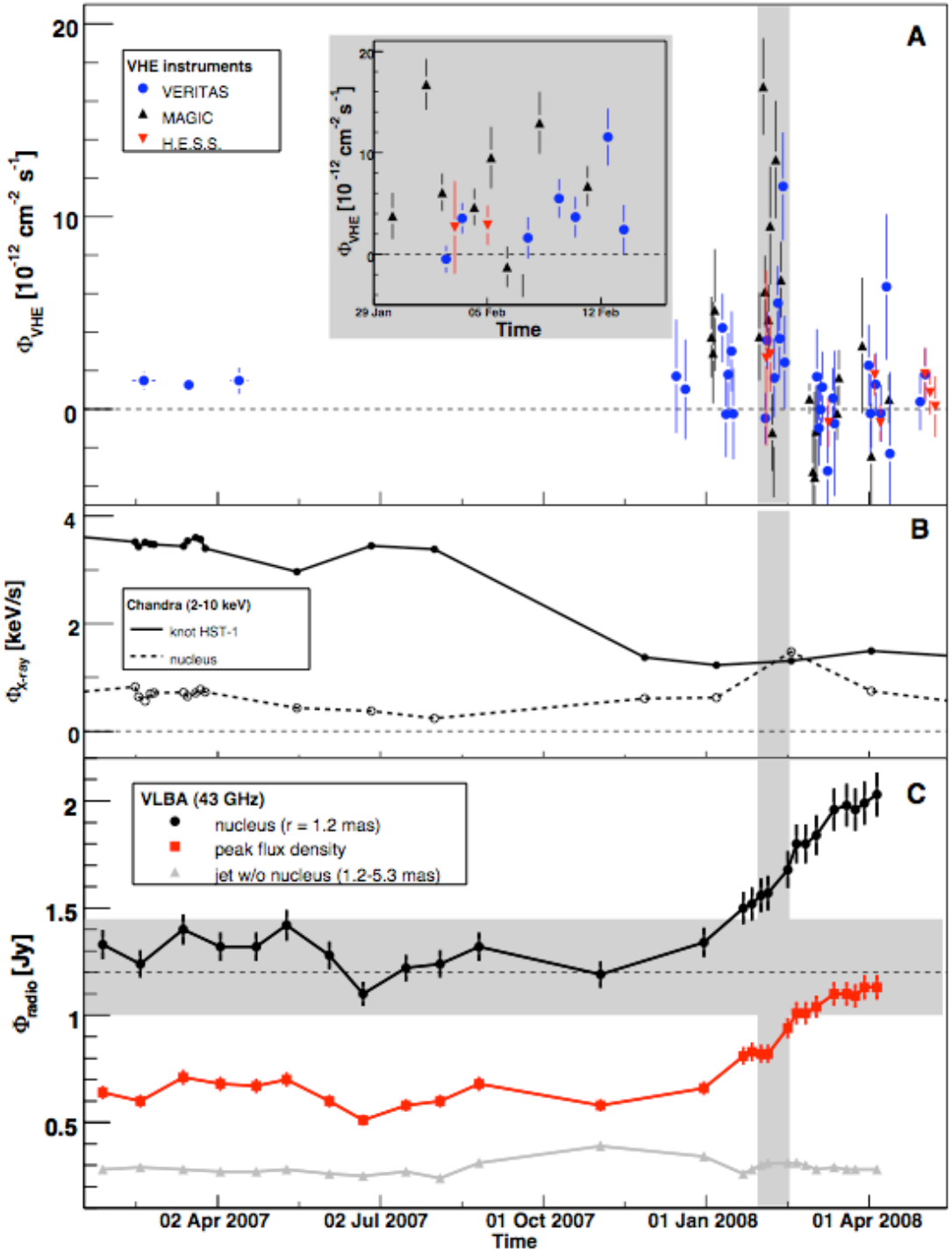

Acciari+ 09

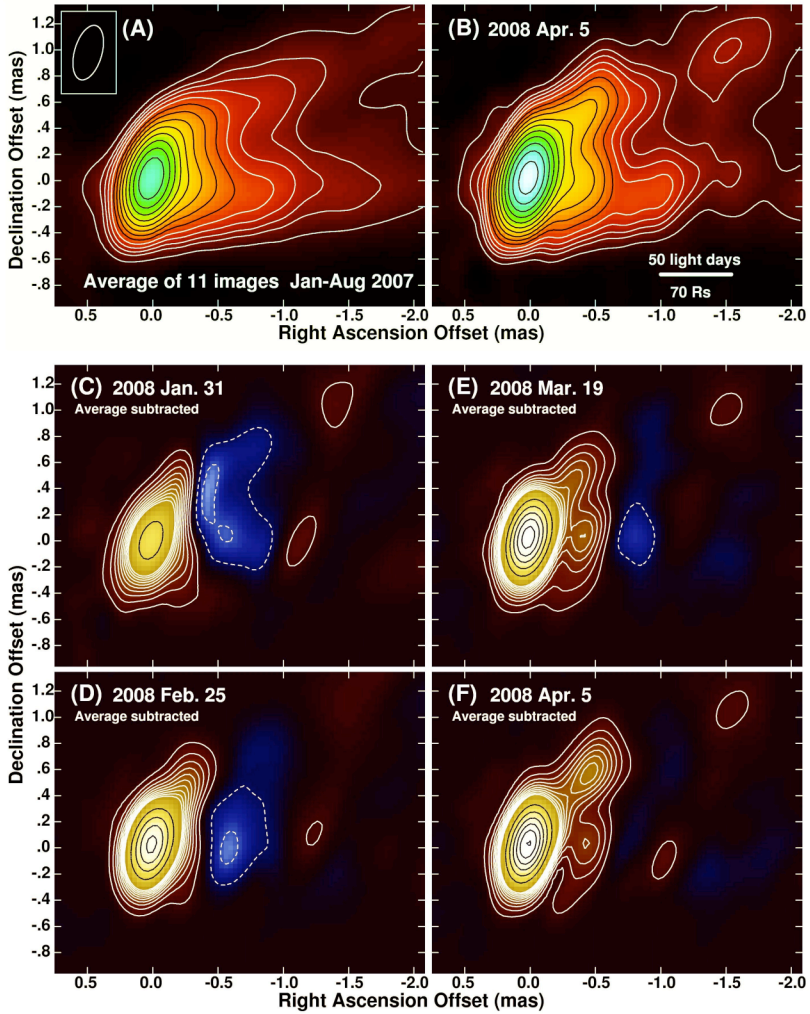

Polarization of pc-Scale Jets

- Radio-to-optical polarization of blazars indicate typically B⊥ for the unresolved cores (especially in the case of BL Lacs), and variety of configurations for the resolved sub-pc scale jets (**Impey+ 91, Cawhorne+ 93, Gabuzda & Sotho 94, Cawthorne & Gabuzda 96, Stevens+ 96, Nartallo+ 98, Gabuzda+ 00, Lister & Homan 05, Jorstad+ 07**).
- B⊥ may indicate compression of the tangled magnetic field by shocks, while B|| shearing of the tangled magnetic field due to velocity gradients (**Laing 80, 81, Hugh+ 89**). This would be consistent with matter-dominated outflows.
- B⊥ could also be due to the dominant toroidal MF. Such interpretation is consistent with B⊥ observed at the spatially extended regions where the jets bend, and also with the observed altering B⊥- B|| structures (**Gabuzda+ 04**).
- Interpretation of the blazar polarization data is complicated and in some cases not conclusive due to the relativistic effects involved (**Lyutikov+ 05**).

Spine-Shear Layer Structure

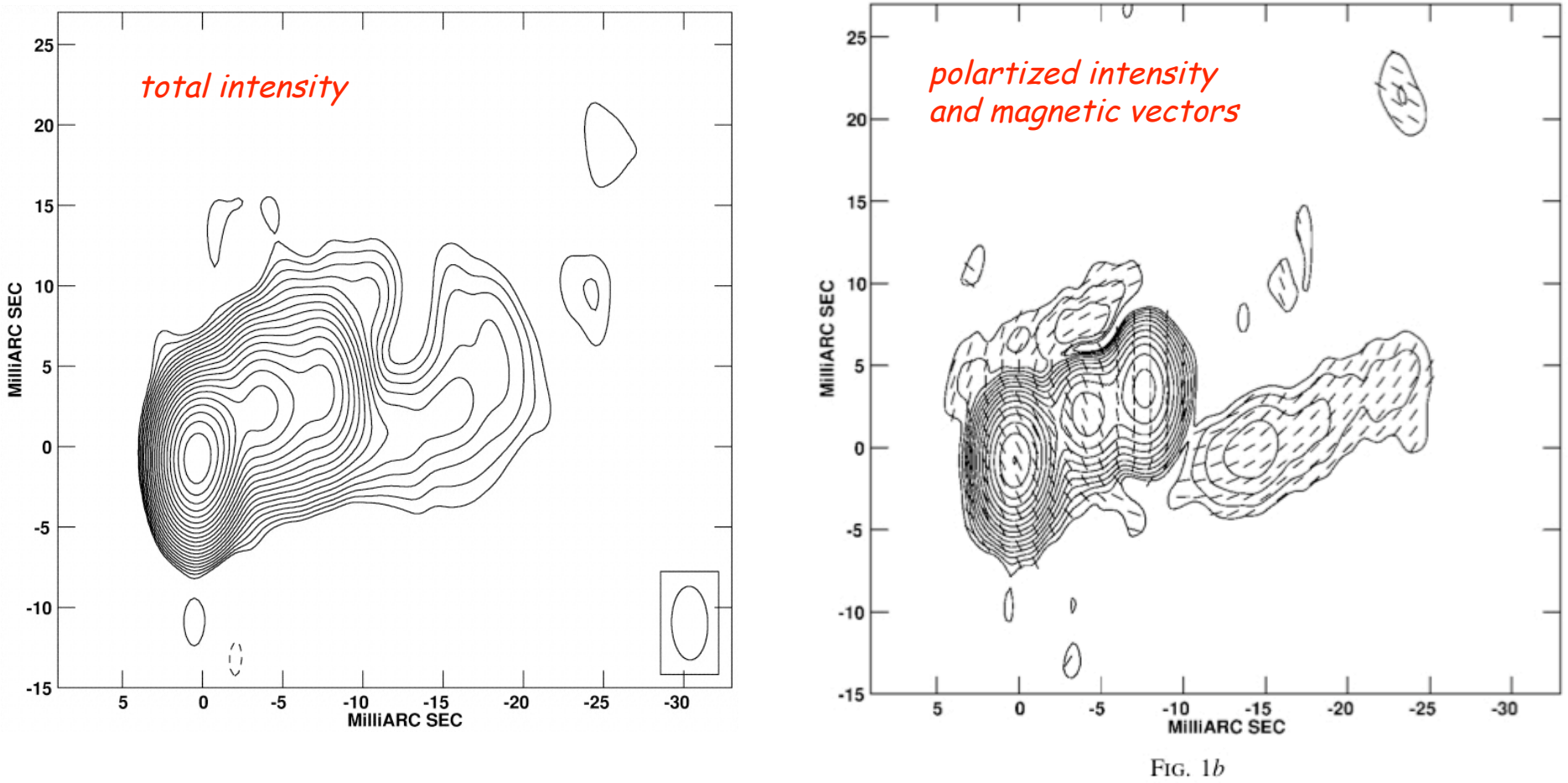

FIG. 1*b*

Attridge+ 99: Spine B⊥ / boundary layer B|| structure in 1055+018.
Shock compression/velocity shear in the matter-dominated jet,
or helical MF in the current-carrying outflow?
(similar cases: **Gabuzda+ 01, Pushkarev+ 05**)

RM Gradients: Expected

$$c^2 k^2 = \zeta \omega^2$$

$$\zeta = 1 - \frac{\omega_{\rm pl}^2}{\omega\,(\omega \pm \omega_{\rm L})}$$

$$v_{\rm ph} = \frac{\omega}{k} \quad , \quad v_{\rm gr} = \frac{\partial \omega}{\partial k}$$

$$\Delta\chi = \frac{2\pi\, e^3}{m_{\rm e}^2 c^2\, \omega^2} \int_0^L n_{\rm th}\, B_{0,\parallel}\, ds$$

$$\left(\frac{\Delta\chi}{\rm rad}\right) = RM \cdot \left(\frac{\lambda}{\rm m}\right)^2$$

$$RM = 0.81 \int_0^L \left(\frac{n_{\rm th}}{\rm cm^{-3}}\right) \left(\frac{B_{0,\parallel}}{\mu\rm G}\right) \left(\frac{ds}{\rm pc}\right)$$

When propagating through a magnetized plasma ("external screen"), a polarized wave experiences rotation of a plane of polarization. That is because any plane polarized wave can be treated as a linear superposition of a right-hand and left-hand circularly polarized component. Circularly polarized wave with positive helicity has different phase velocity than the wave with negative helicity within the magnetized environment.

Gabuzda 06

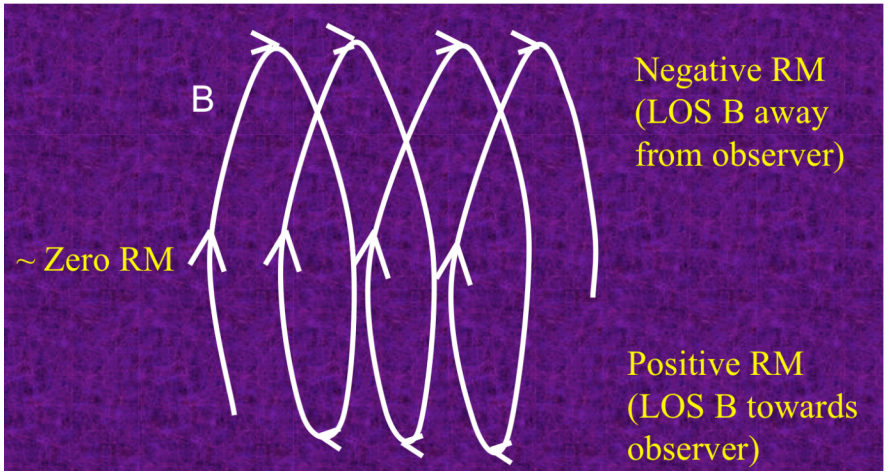

RM gradients across a jet should be expected in the case of a helical magnetic field (**Blandford 93**)

RM Gradients: Observed

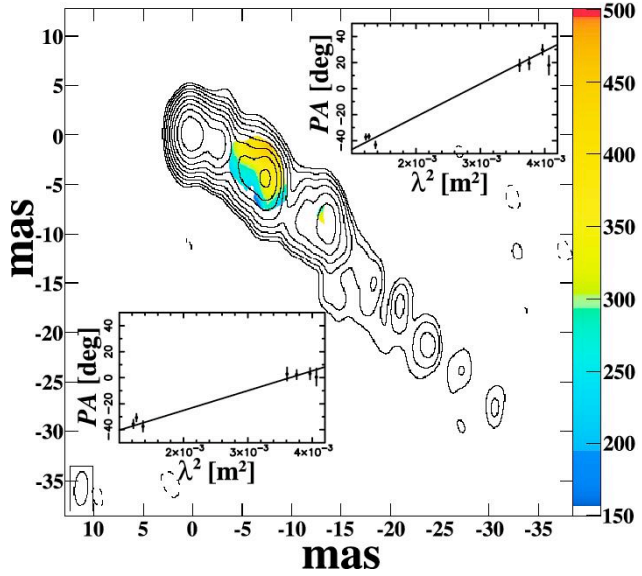

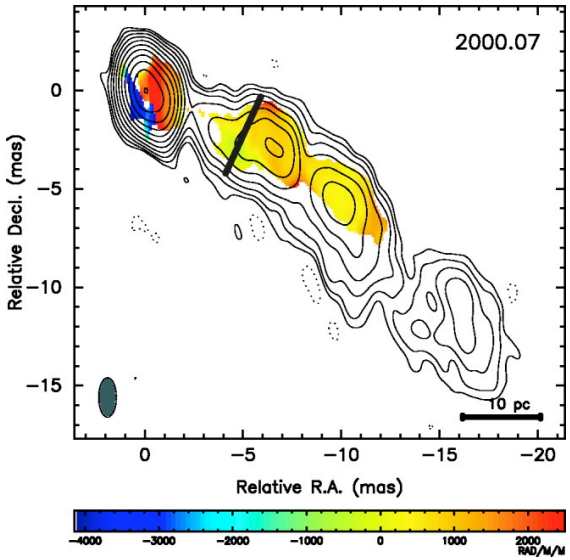

3C 273:
Asada+ 02, 08, Zavala & Taylor 05

(many other examples:
Gabuzda+ 04, 07, 08)

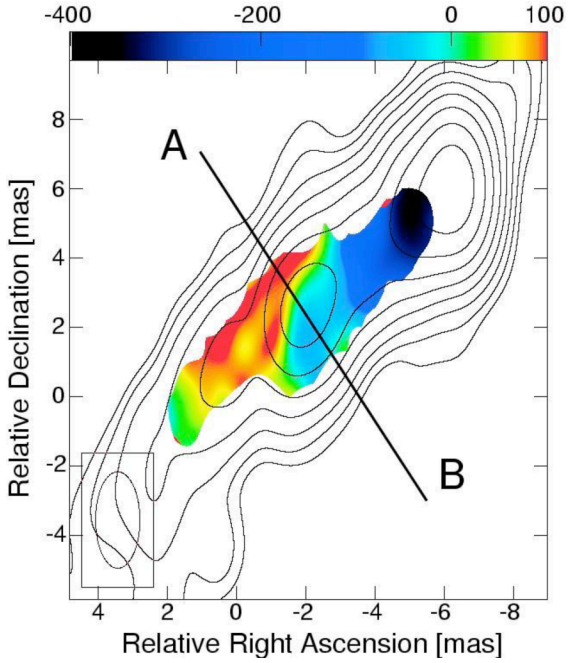

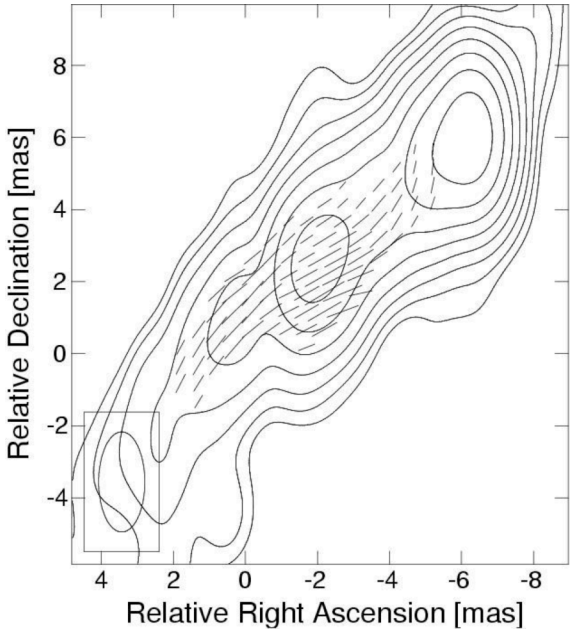

Asada+ 08: B|| polarization structure in NRAO 140 together with strong RM gradient suggest loosely wound magnetic helix in a jet spine (where most of the radio emission is produced), and tightly wound magnetic helix in an outer sheath (which acts as a Faraday Screen).

Where Is Faraday Screen?

Faraday screen has to be external to the emitting region because:

- Rotations >45deg sometimes observed (**Sikora+ 05**).
- RM gradients sometimes localized where the jet interacts with the clouds of ISM (3C 120; **Gomez+ 00,08**).
- λ^2 dependence always holds.
- Decrease of RM along the jets observed (**Zavala & Taylor 02,03,04**).
- High fractional polarization observed from the RM gradient regions.

Faraday screen cannot be completely unrelated to jet because:

- RM gradients vary on timescale of years (**Zavala & Taylor 05, Asada+ 05**).
- Direction of RM gradients always agrees with a sign of a circular polarization observed (**Gabuzda+ 08**)*.

Spine/Sheath structure again?

**CP may result from Faraday conversion of LP mediated by helical MF. The sign of CP is then determined by the helicity of MF, and so should agree with the direction of the RM gradient.*

Magnetic Field at Large Scales

- In the case of a matter-dominated jet, when the MF is frozen-in to the fluid, one expects $B_T \propto r^{-1}$ and $B_P \propto r^{-2}$ (conservation of MF energy flux and MF flux; **Begelman+ 84**). Thus, the toroidal MF should dominate over the poloidal one on large scales. This simple scalling is roughly consistent with the equipartition MF intensity:

$B_{eq} \sim B \sim B_{blaz}\,(pc/100kpc) \sim B_E\,(r_g/100kpc) \sim 1\text{-}10\mu G$

- However, polarimetry of large-scale jets in powerful quasars and radio galaxies indicate B||. This may suggest action of a velocity shear (re)-orienting MF lines (**Laing 80, 81**). The regions with strong velocity shear are likely to be the sites of the enhanced magnetic reconnection, dynamo action, and injection of turbulence, and therefore of the enhanced particle acceleration/energy dissipation (**De Young 86**).
- Note that the longitudinal MF component cannot be unidirectional on large scales, since this would imply too large magnetic flux: $B_{eq}\,(kpc)^2 \gg B_E\,r_g^{\,2}$. Thus, B|| must indeed reverse many times across the jet (**Begelman+ 84**).

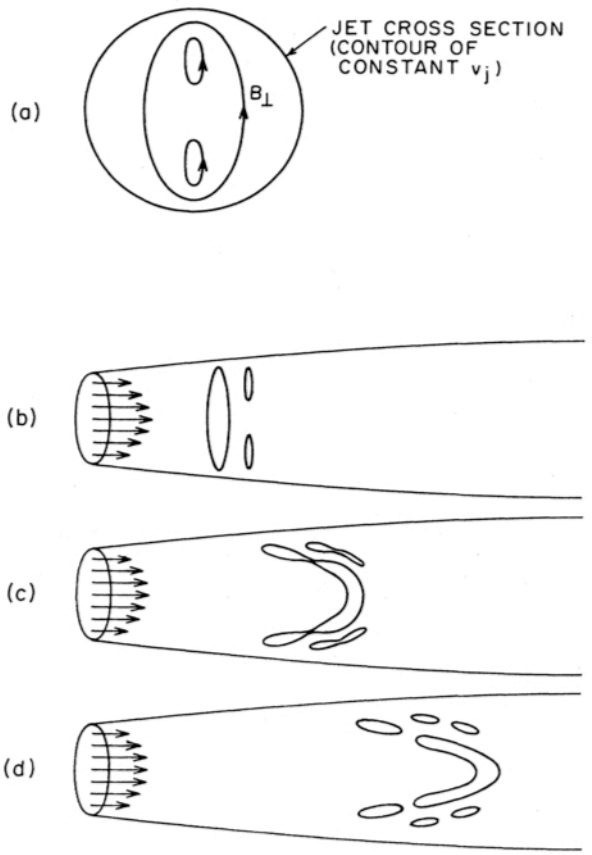

Begelman+ 84

Observed MF Structure

- **Laing & Bridle 02,04** proposed "decelerating adiabatic" model for 3C 31 jet: radiating particles are accelerated before entering the region of interest and then lose energy only by the adiabatic losses, while the MF is frozen into and convected passively with the flow".
- It was found that while the intensity distribution can be reproduced well in this model, the polarization data cannot be explained. The departures from adiabatic conditions in the 3C 31 jet suggest deviation from the flux-freezing condition and efficient in-situ particle acceleration (as required by the X-ray data).
- **Canvin & Laing 04, Canvin+ 05** relaxed the adiabatic condition, and provided good fits to several FR I jets (both intensity and polarization data; e.g., NGC 315).

MF is modeled as random on small scales but anisotropic. Globally ordered helical configuration is excluded.

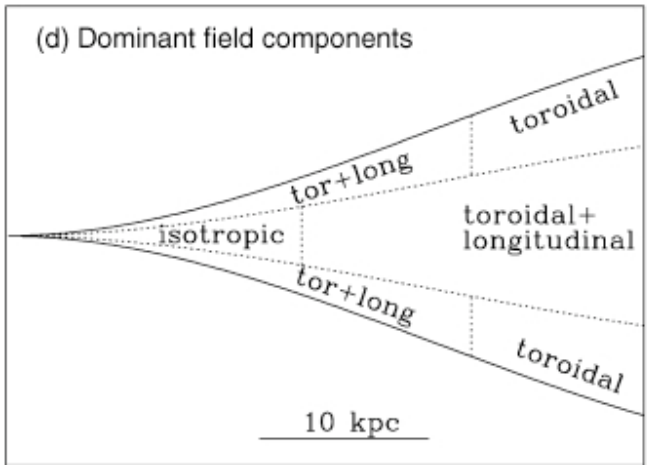

Laing+ 08: 3C 31 as an archetype of FR I jets

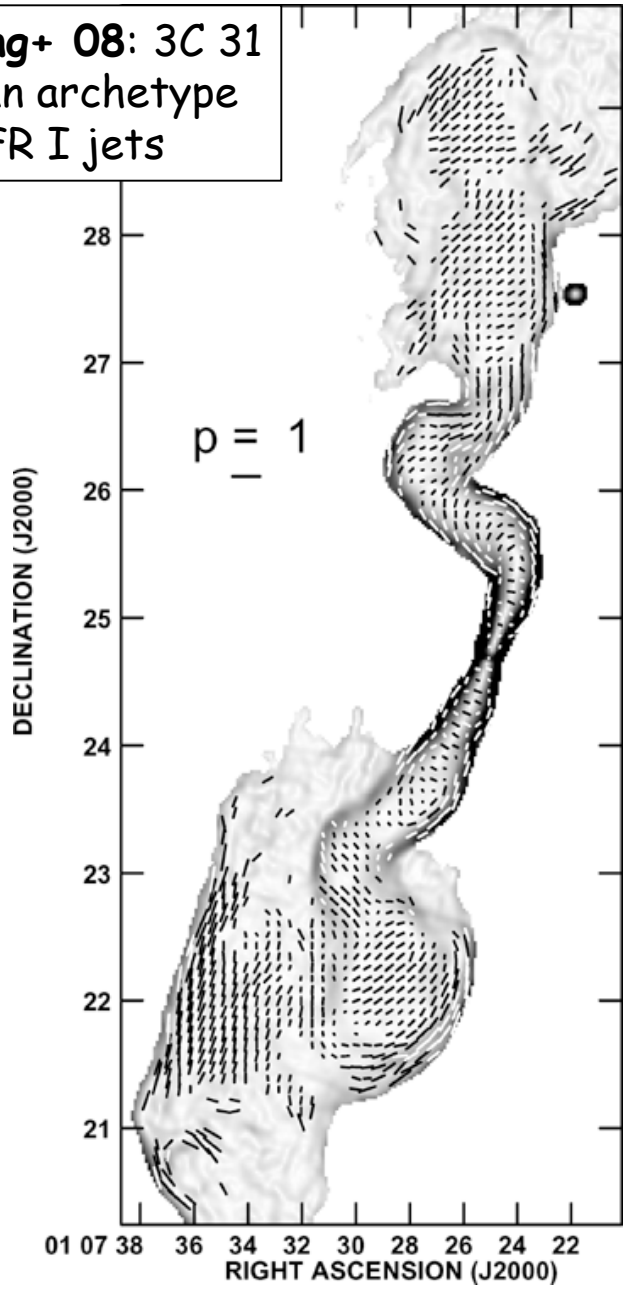

FR I Jets

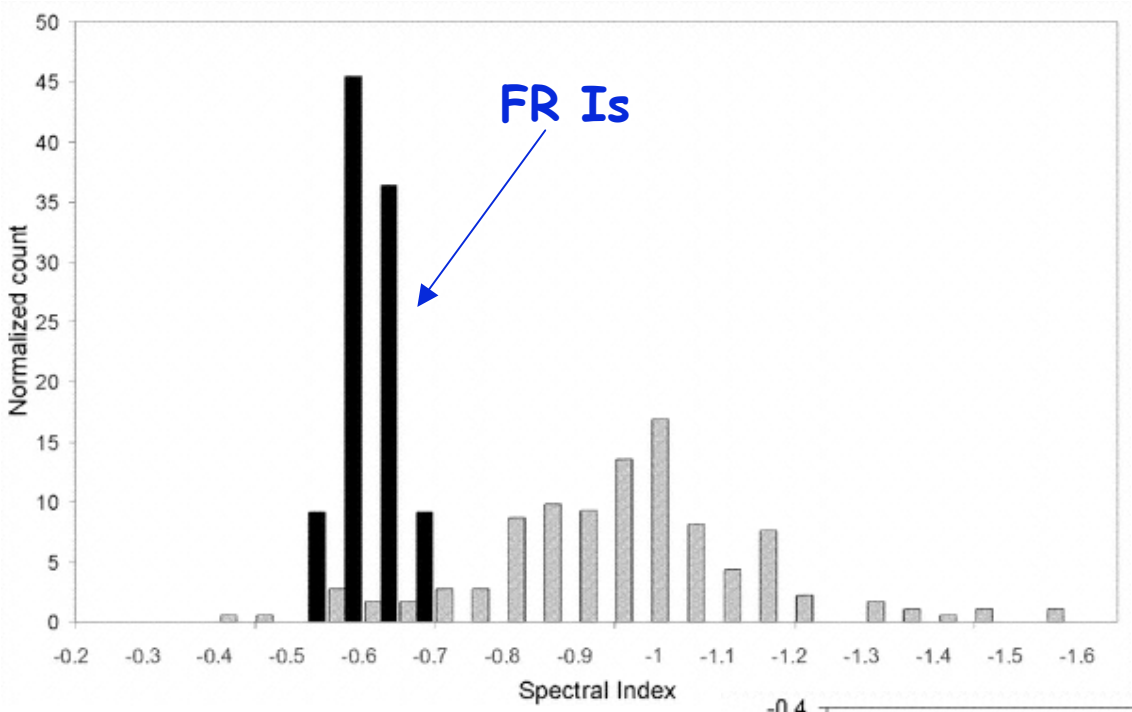

Young+ 05:

Canonical radio spectral index of FR I jets, α_R = 0.55, implying universal particle spectrum n(E) $\propto E^{-2.1}$

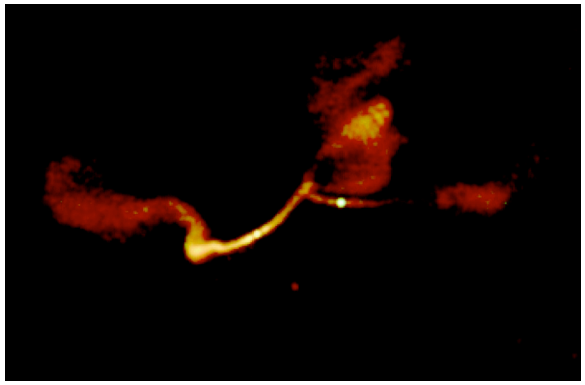

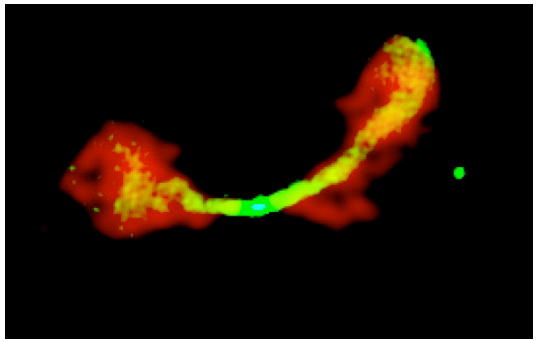

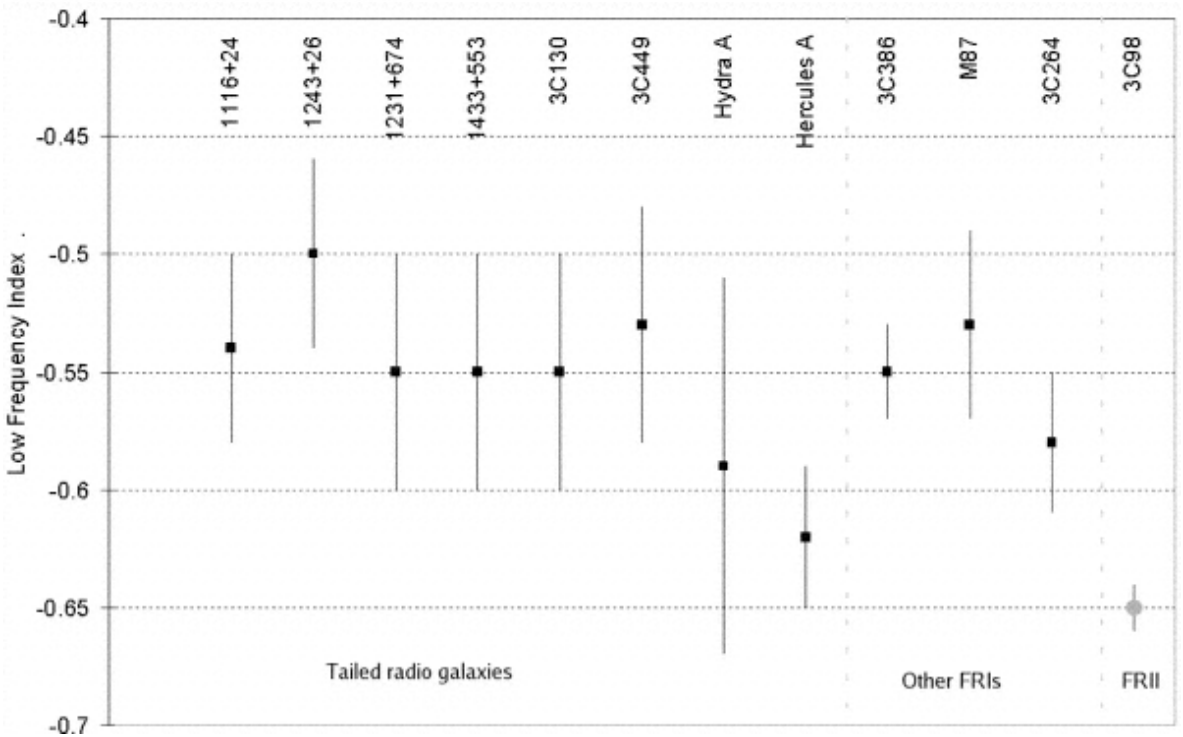

M 87

2-kpc-long jet in M87 radio galaxy (d_L = 16 Mpc) observed at radio, optical, and X-ray frequencies. Polarization structure consistent with the spine – boundary shear layer morphology, and so matter-dominated outflow (**Perlman+ 99**).

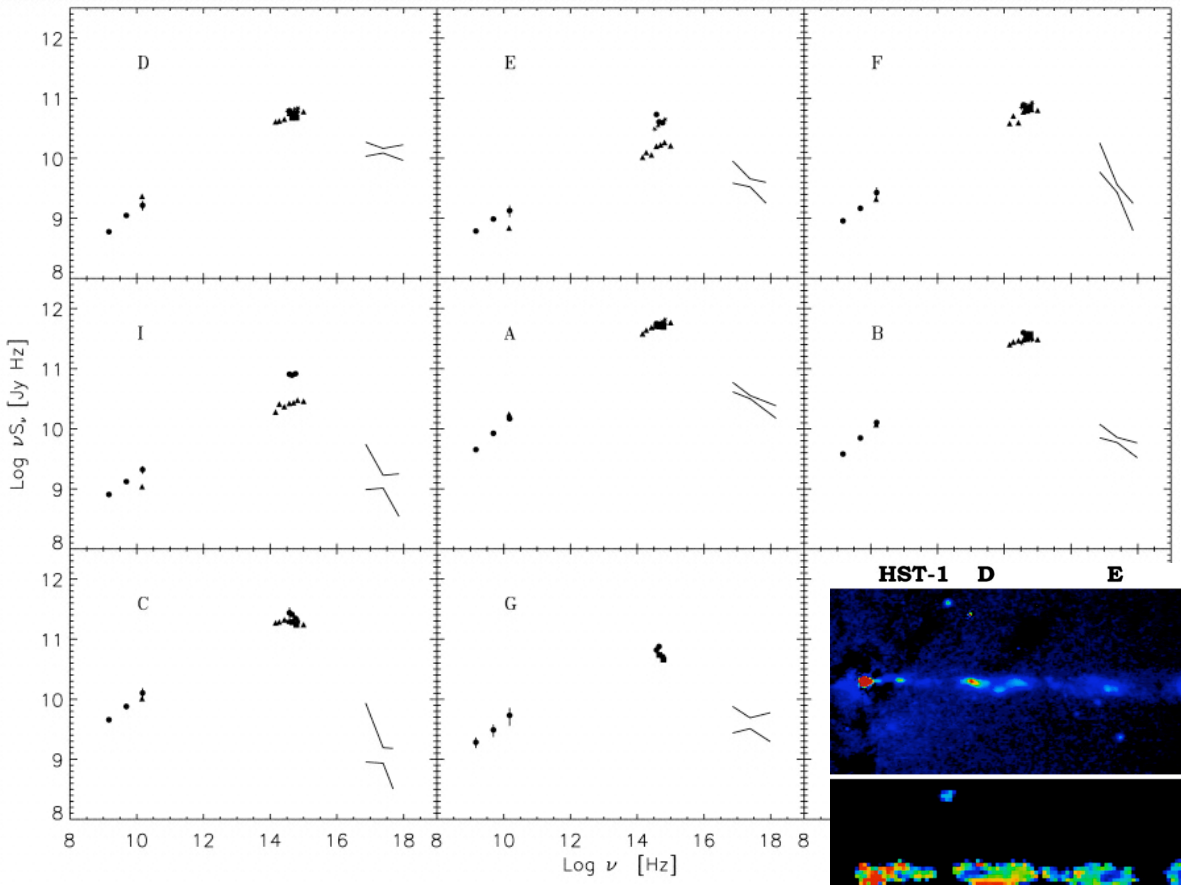

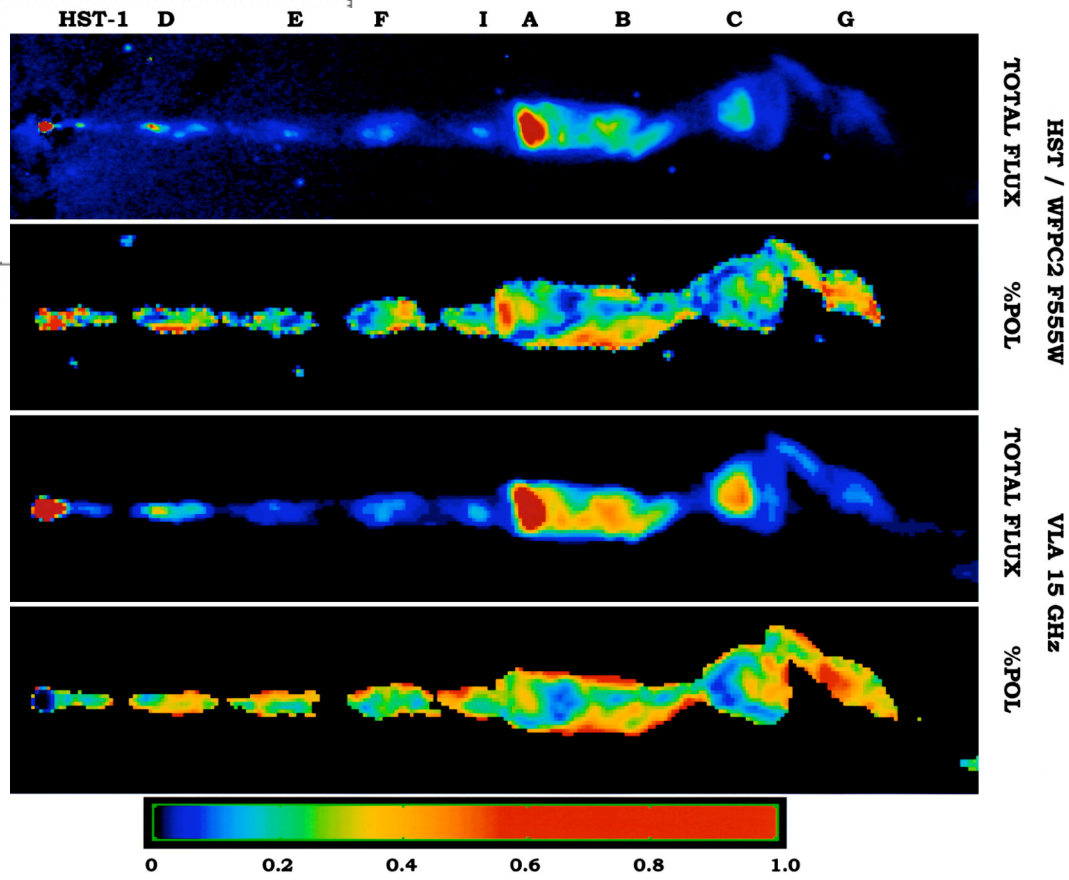

Radio-to-X-ray synchrotron emission:
- presence of 100 TeV energy electrons;
- broad-band knots' spectra hardly consistent with the "standard" cooled power-laws; need for continuous electron acceleration along the whole jet ($\ell_X \sim 10$ pc « 2 kpc).

Marshall+ 02, Wilson & Young 02, Wilson & Perlman 05)

How Strong Magnetic Field?

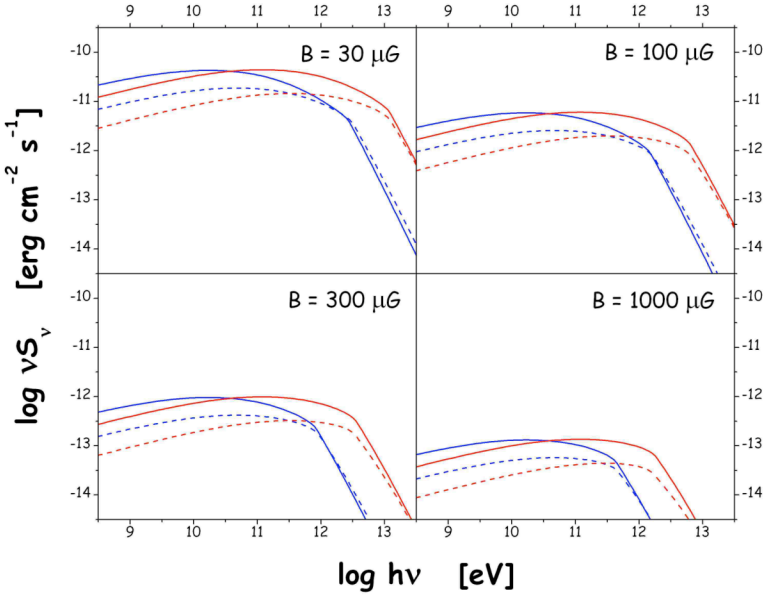

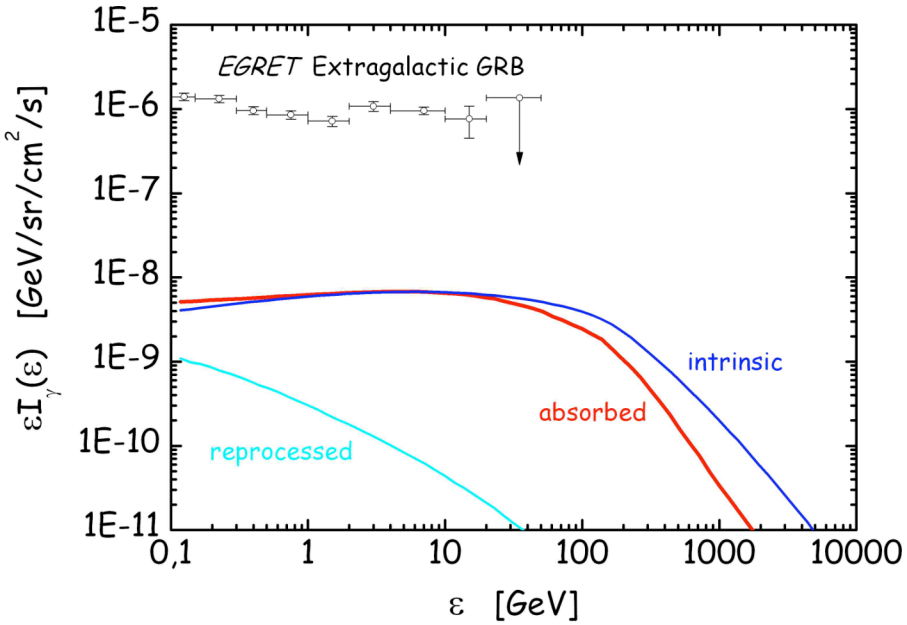

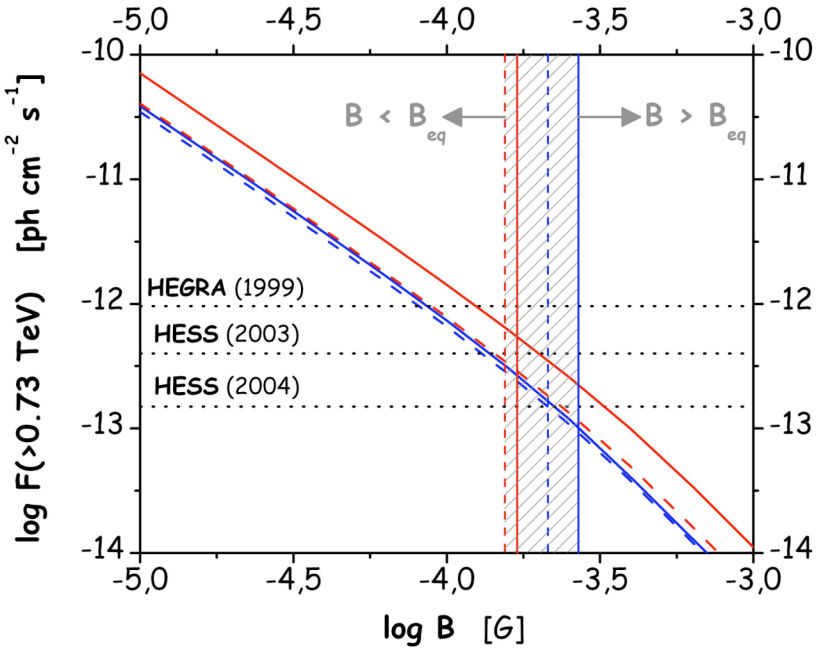

LS+ 05: analysis of the expected TeV emission of kpc-scale jet in M87 radio galaxy, when compared with the HESS observations, indicate strong magnetic field $B \geq B_{eq}$.

LS+ 06: similar analysis performed for the whole FR I population, compared with the extragalactic EGRET gamma-ray backround, indicates $B > 0.1\ B_{eq}$ on average in kpc-scale FR I jets.

Fermi/LAT will provide stronger constrains!

Centaurus A

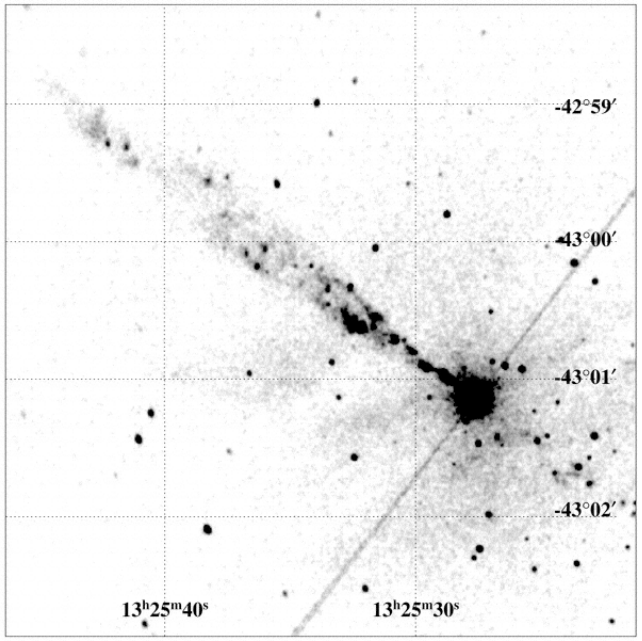

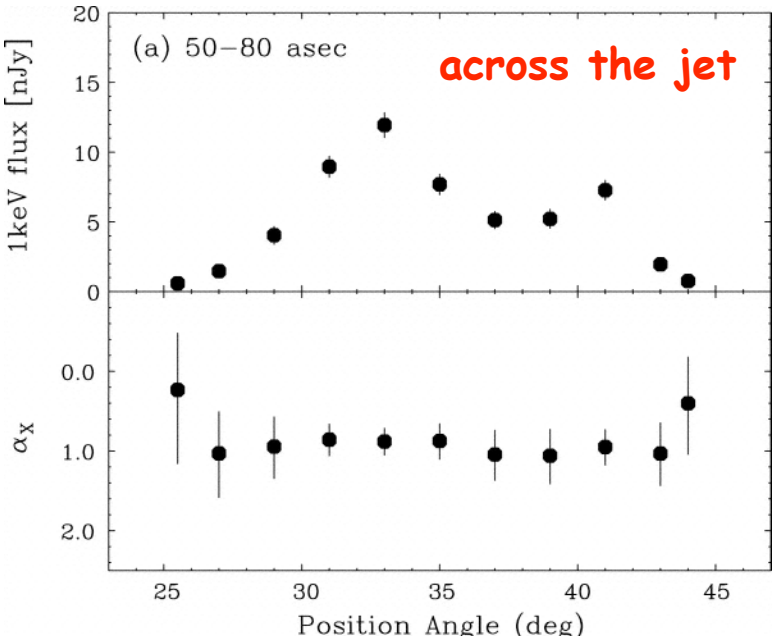

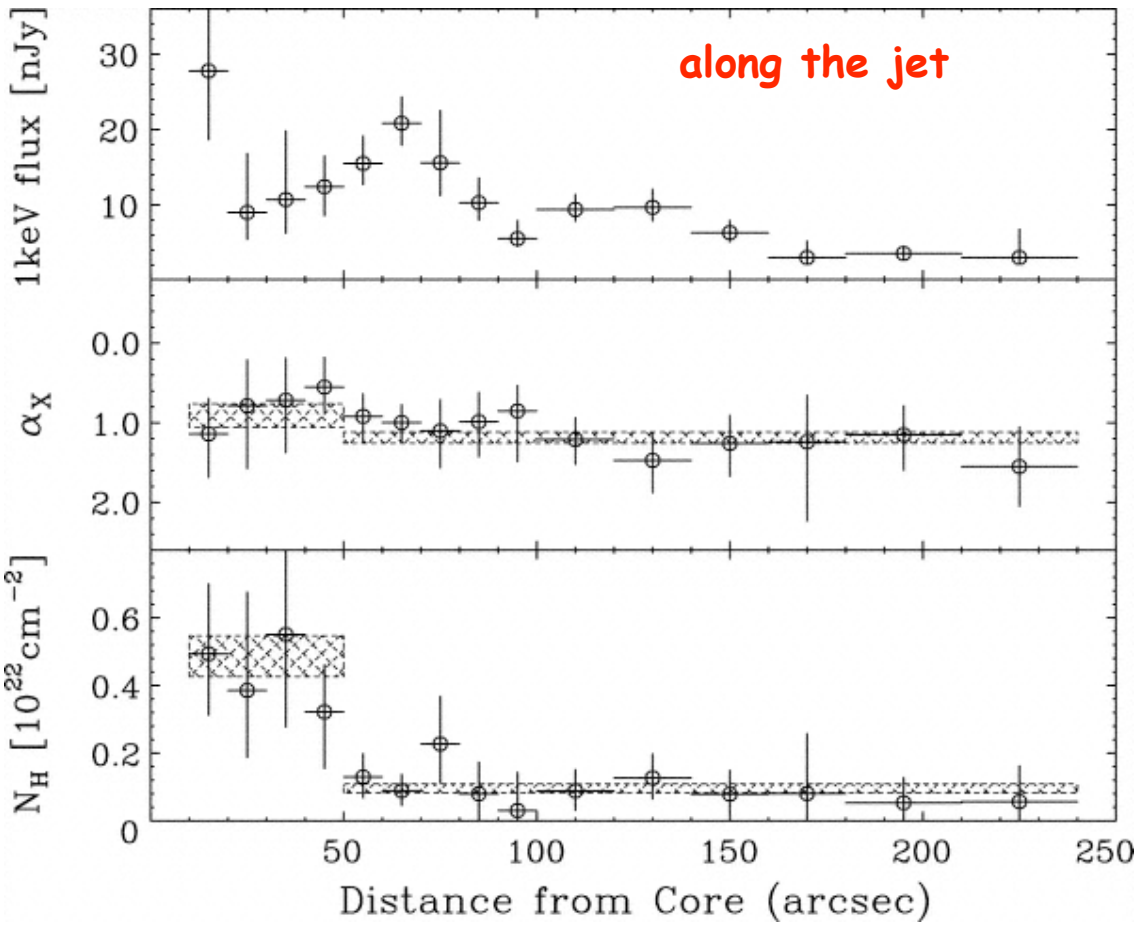

Kataoka+ 06: Diffuse X-ray emission of 4 kpc-scale X-ray jet in Centaurus A radio galaxy is characterized by a uniform and constant spectral index $\alpha_X = 1$

Chandra Quasar Jets

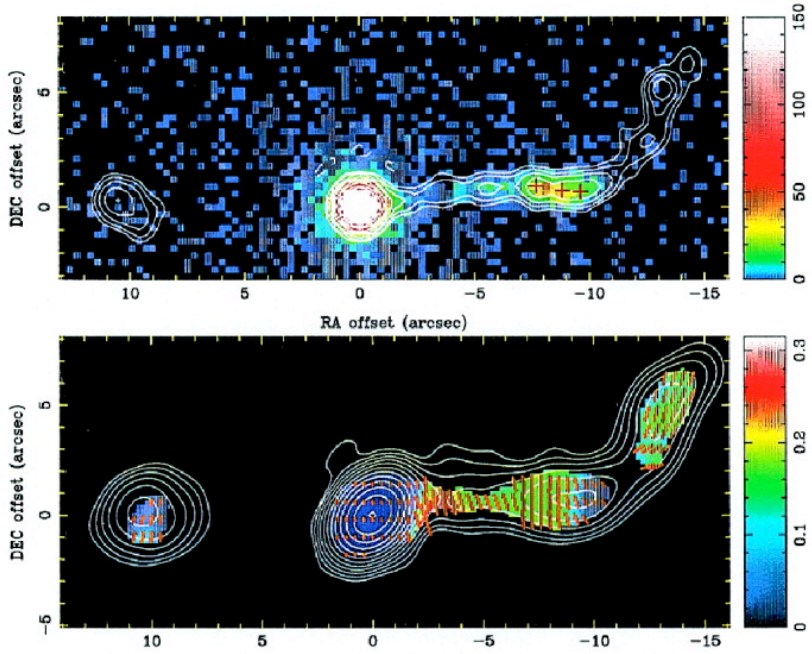

Chandra X-ray Observatory detected surprisingly intense X-ray emission from large-scale (100 kpc – 1 Mpc) quasar jets (L_X ~ 10^{44}-10^{45} erg/s).

Many examples (e.g., **Schwartz+ 00, Cheung+, Hardcatle+, Harris+, Jorstad+, Kataoka+, Kraft+, Marshall+, Sambruna+, Siemiginowska+**).

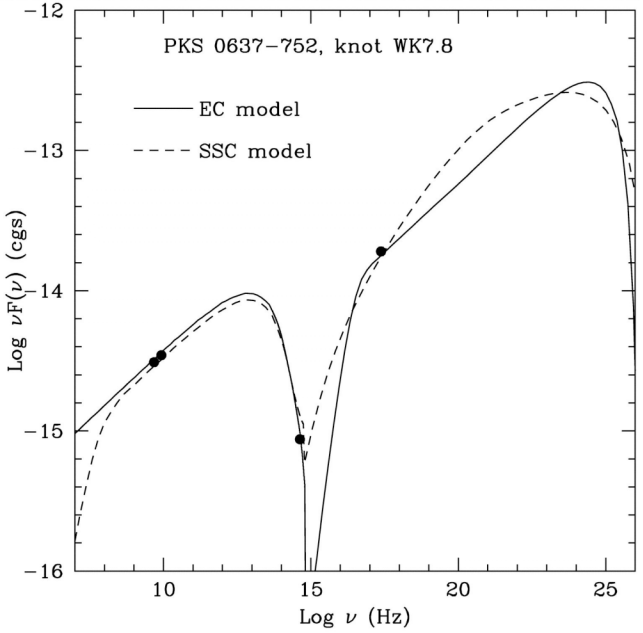

It was proposed that this X-ray emission is due to inverse-Compton scattering of the CMB photons by low-energy jet electrons, E_e ~ 10-100 MeV. (**Tavecchio+ 00, Celotti+ 01**).

IC/CMB model requires highly relativistic bulk velocities ($\Gamma > 10$) on Mpc scales, and dynamically dominating protons,

$L_p > L_e \sim L_B$

with $B \sim B_{eq}$ ~ 1-10 μG.

X-ray Jets at High Redshifts

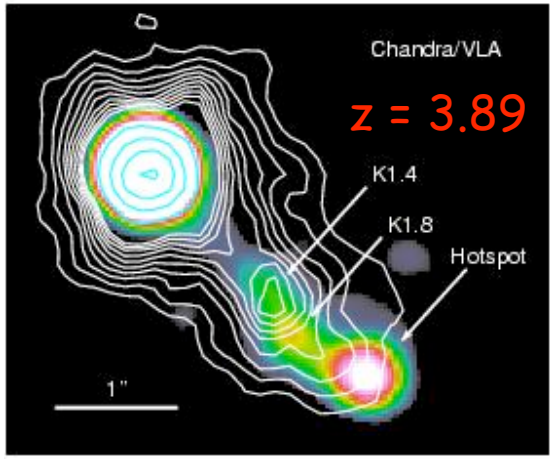

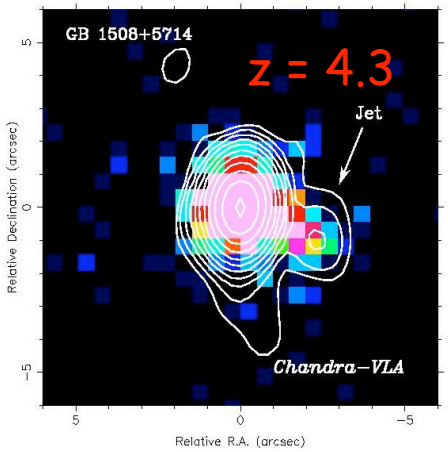

(Siemiginowska+ 03, Cheung 04, Cheung+ 06, 09)

$L_{ic/cmb} = (\delta/\Gamma)^2 \times (U'_{cmb}/U'_B) \times L_{syn}$

$U'_{cmb} = 4 \times 10^{-13} (1+z)^4 \Gamma^2$ erg/cm^3

$U_{cmb} \propto (1+z)^4 \Rightarrow$

if the IC/CMB model is correct, then one should expect

- an increase in the X-ray core luminosity with redshift due to unresolved portion of the jet;
- $L_X/L_R \propto (1+z)^4$ for the resolved portion of the jet.

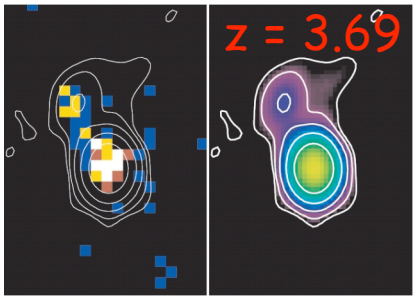

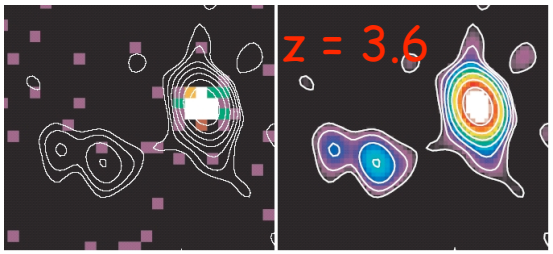

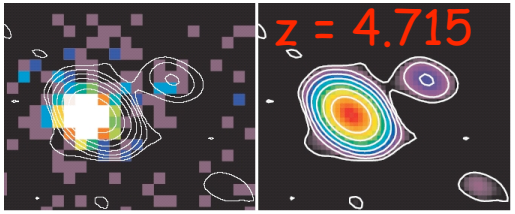

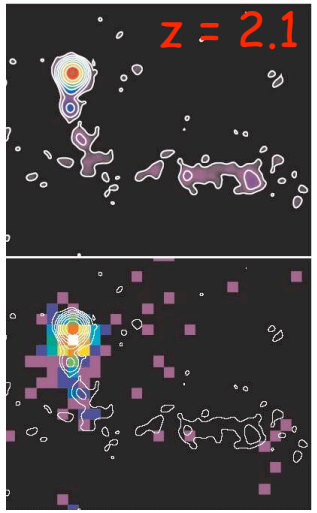

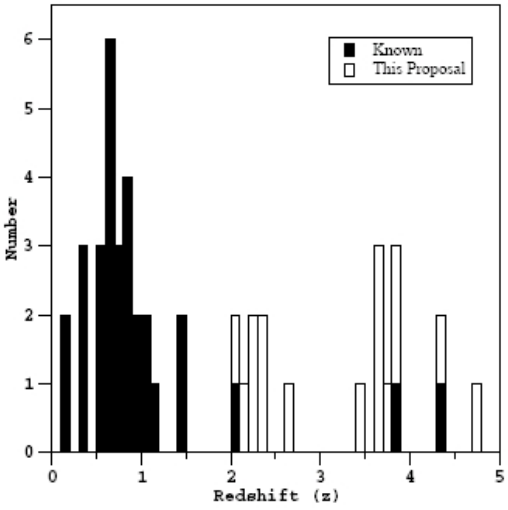

3C 353

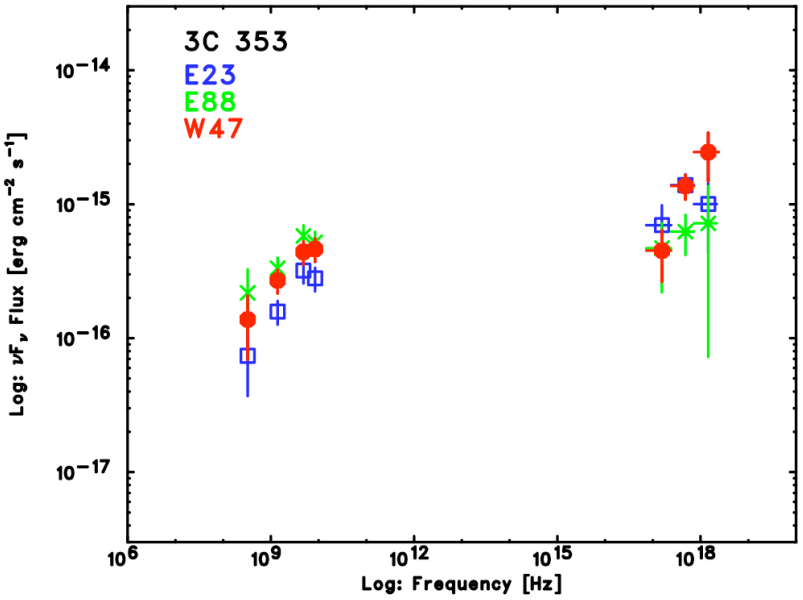

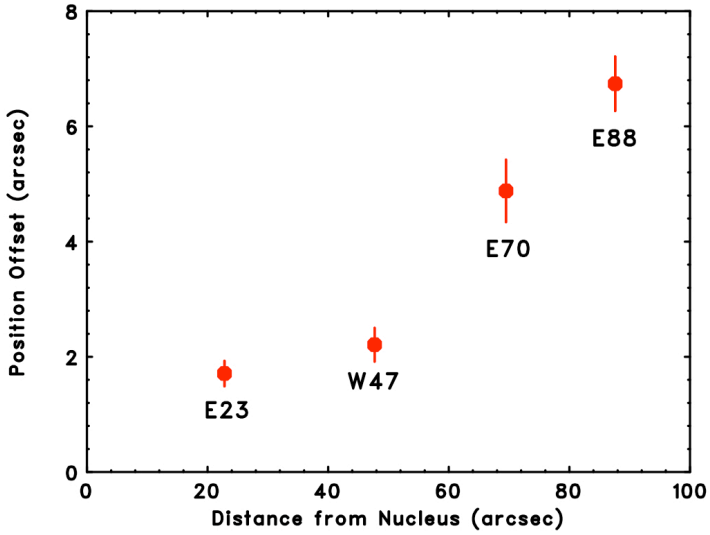

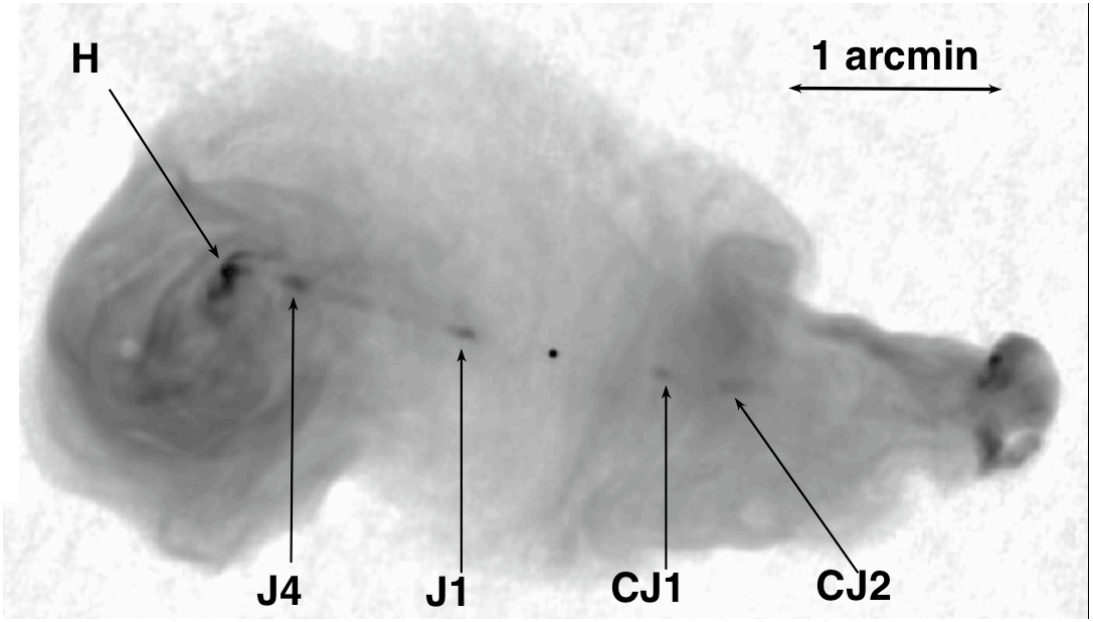

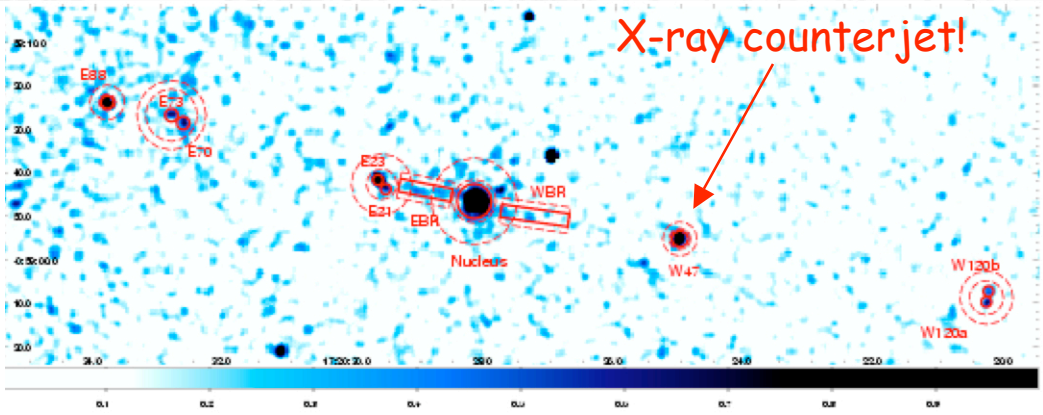

The detection of the X-ray counterjet in FR II radio galaxy 3C 353 (**Kataoka+ 08**), plus X-ray/radio profiles along the jets and offsets between the positions of radio and X-ray knots indicate that the IC/CMB scenario for the X-ray emission of Chandra quasar jets may not be the case (see also quasar PKS 1127, **Siemiginowska+ 07**).

Non-standard Electron Spectra?

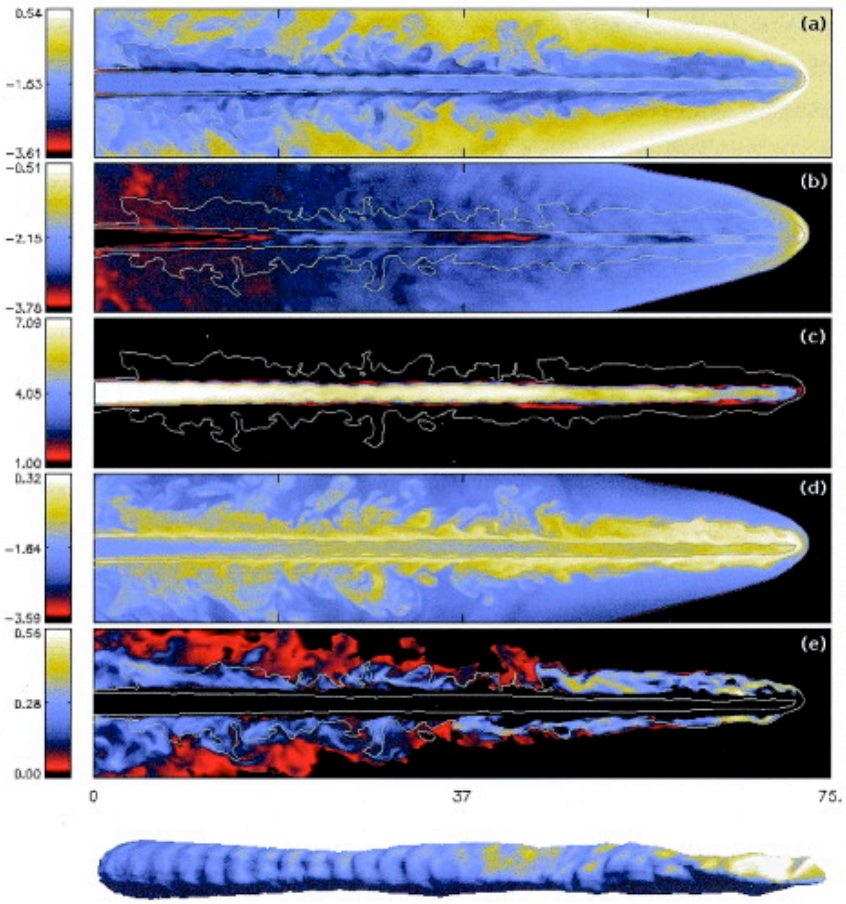

Relativistic 3D-HD simulations indicate presence of highly turbulent shear boundary layers surrounding relativistic jets **(Aloy+ 99)**.

Relativistic large-scale jets are highly turbulent, and velocities of turbulent modes thereby may be high. As a result, stochastic (2nd order Fermi) acceleration processes may be dominant. Assuming efficient Bohm diffusion (i.e. turbulence spectrum $\delta B^2(k) \propto k^{-1}$), one has

$$t_{acc} \sim (r_g/c)\,(c/v_A)^2 \sim 10^3\,\gamma \;\; [s]$$
$$t_{esc} \sim R_j^{\,2}/\kappa \sim 10^{25}\,\gamma^{-1} \;\; [s]$$
$$t_{rad} \sim 6\pi m_e c \,/\, \sigma_T\,\gamma B^2 \sim 10^{19}\,\gamma^{-1} \;\; [s]$$

$$r_g \sim \gamma m_e c^2 / eB\,, \quad \kappa \sim r_g c / 3\,,$$
$$v_A \sim 10^8 \text{ cm/s}\,,$$
$$B \sim 10\ \mu G\,, \quad R_j \sim 1 \text{ kpc}\,.$$

$$t_{esc}/t_{rad} \sim 10^6$$
$$t_{acc} \sim t_{rad} \quad \text{for} \quad E_{eq} \sim 100 \text{ TeV}$$

Pile-up synchrotron X-ray emission expected!
(LS & Ostrowski 02, LS+ 04)

3C 273

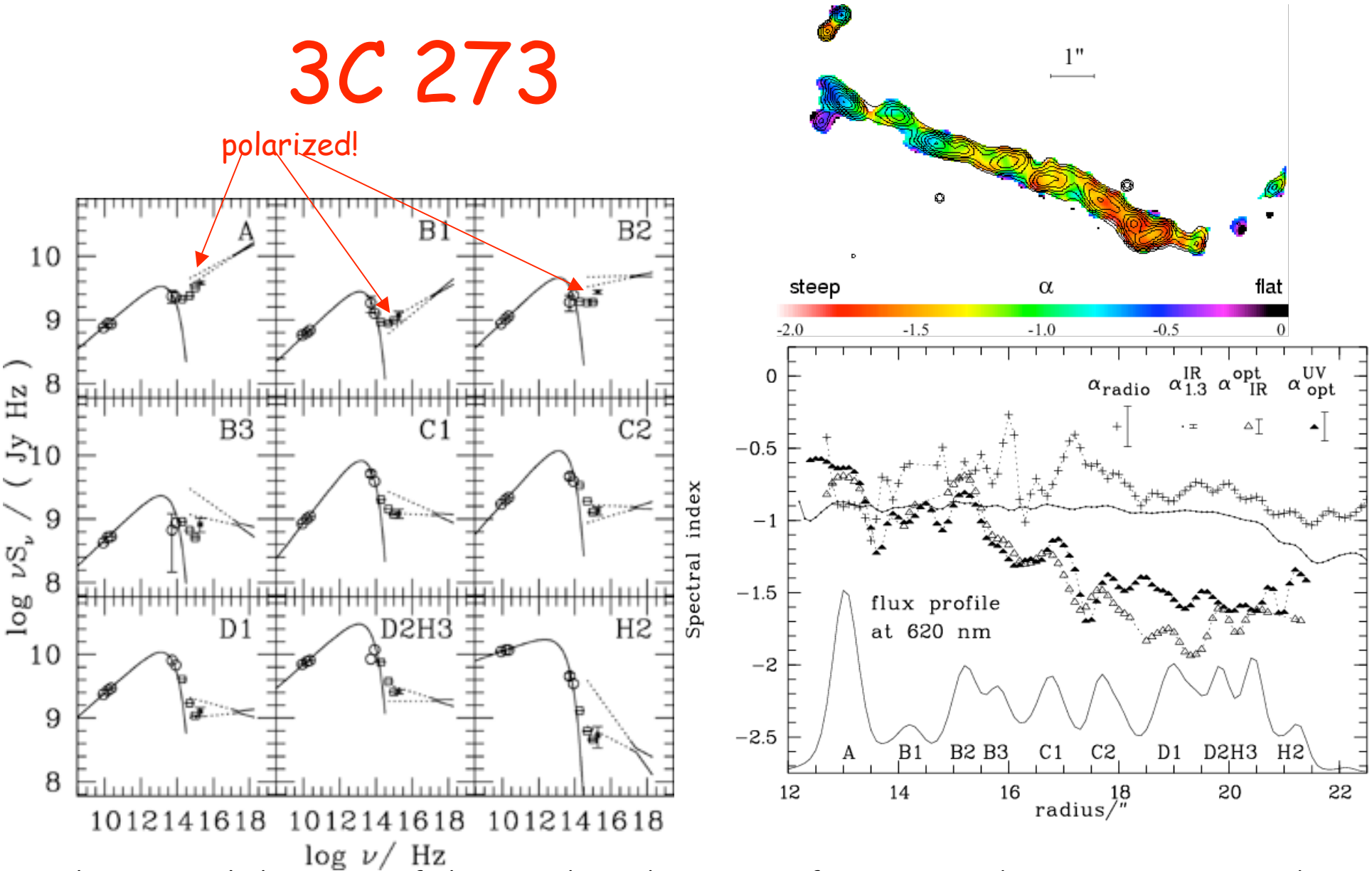

The spectral character of the broad-band emission of 3C 273 jet (**Jester+ 02, 04, 07**), indicates that the synchrotron scenario for the X-ray emission of Chandra quasar jets may be more likely than the IC/CMB model. In such a case, the jet MF may be as well stronger than or equal to the equipartition value. Spectral profile inconsistent with the shock scenario.

Terminal Hotspots

Kino & Takahara 04

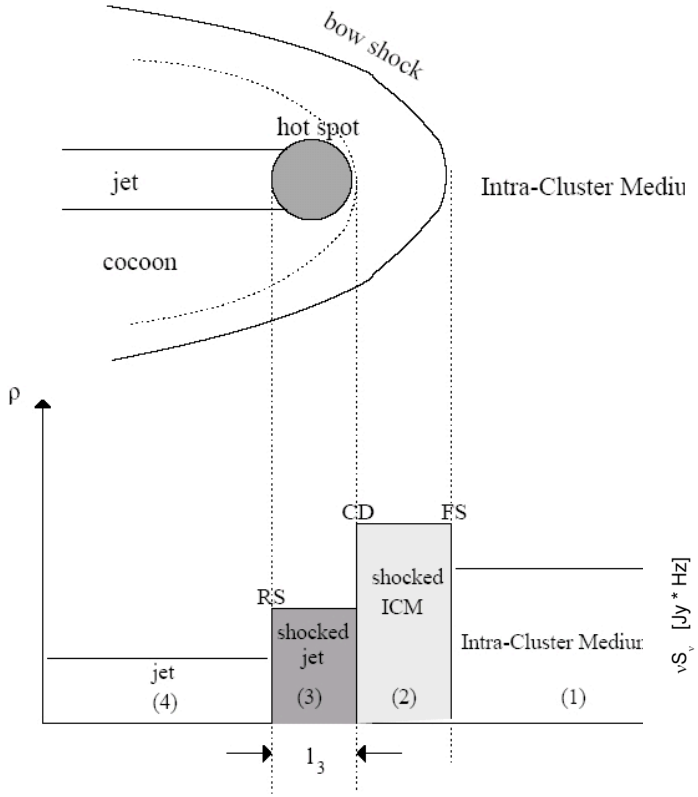

Hotspots in powerful radio sources are understood as the terminal regions of relativistic jets, where bulk kinetic power transported by the outflows from the active centers is converted at a strong shock (formed due to the interaction of the jet with the ambient gaseous medium) to the internal energy of the jet plasma.

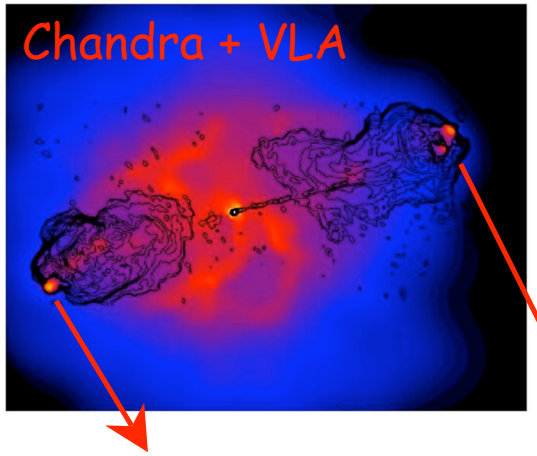

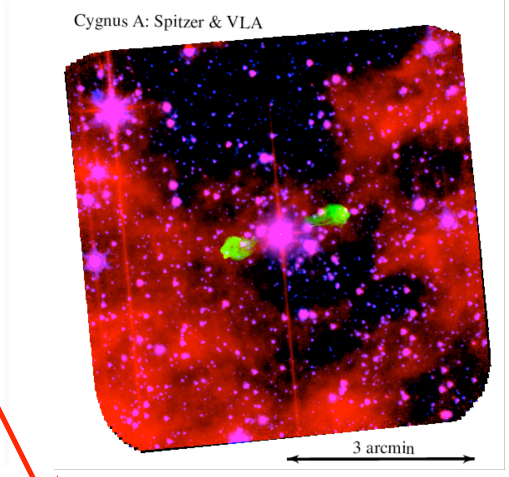

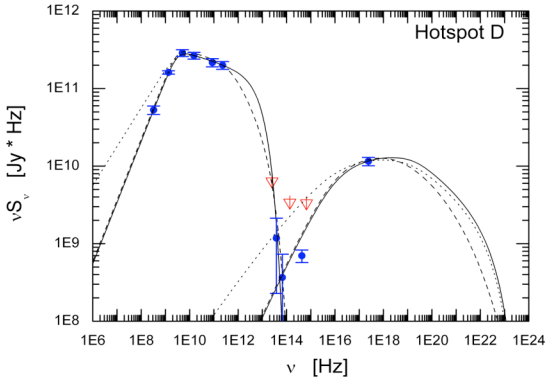

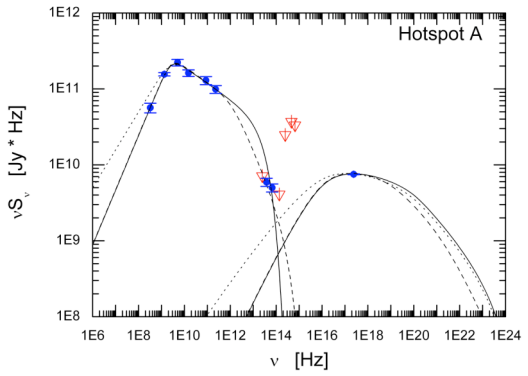

Hotspots of exceptionally bright radio galaxy Cygnus A (d_L = 250 Mpc) can be resolved at different frequencies (VLA, Spitzer, Chandra), enabling us to understand how (mildly) relativistic shocks work **(LS+ 07)**.

Shocks!

LS+ 07: analysis of the broad-band emission of hotspots in the exceptionally bright radio galaxy Cygnus A indicates $U_B \sim U_e$ and terminal shocks dynamically dominated by protons.

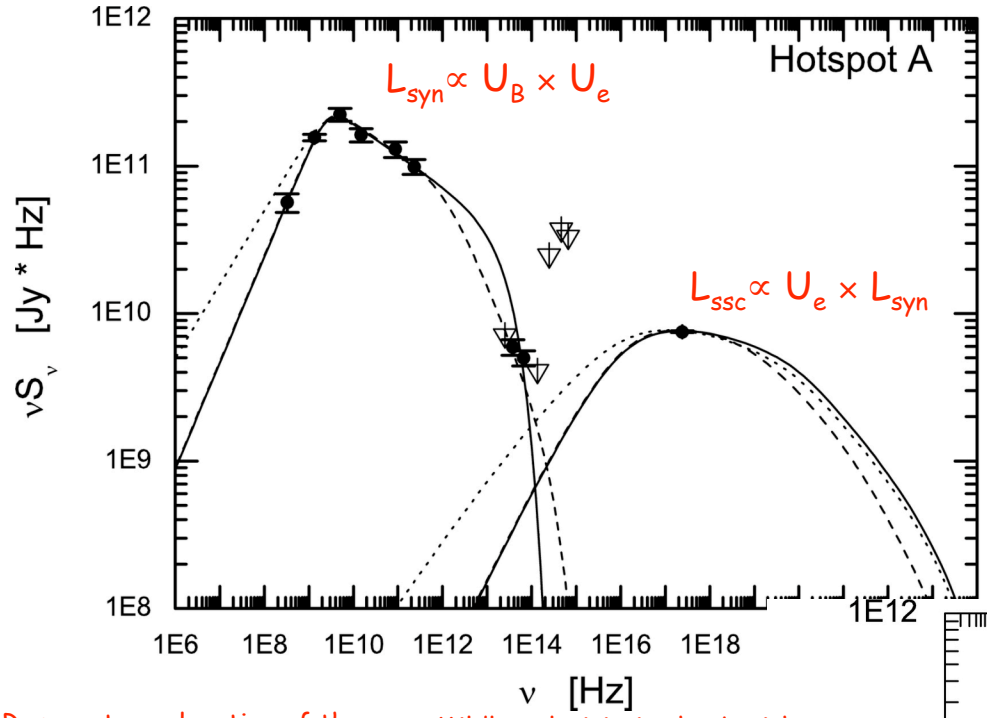

Resonant acceleration of the type discussed by **Hoshino+92** **Amato & Arons 07**

Mildly-relativistic shock with perpendicular MF results in a Steep particle spectrum: **Niemiec & Ostrowski 04**

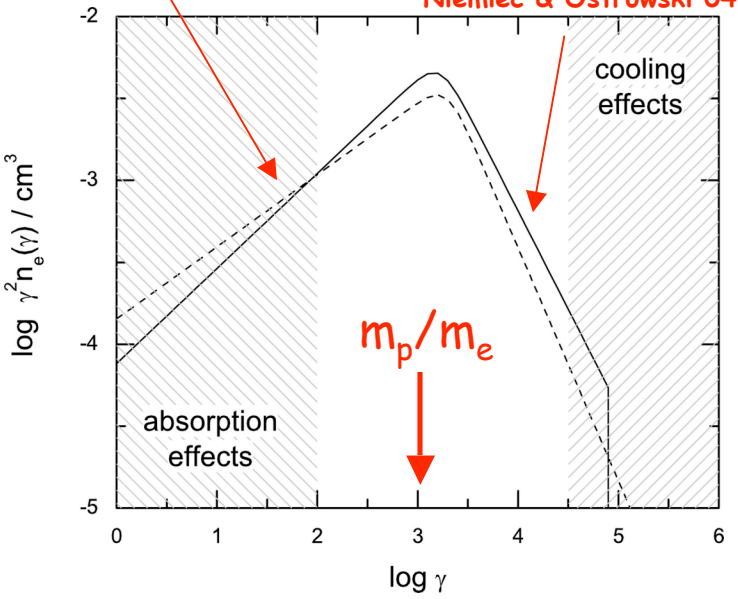

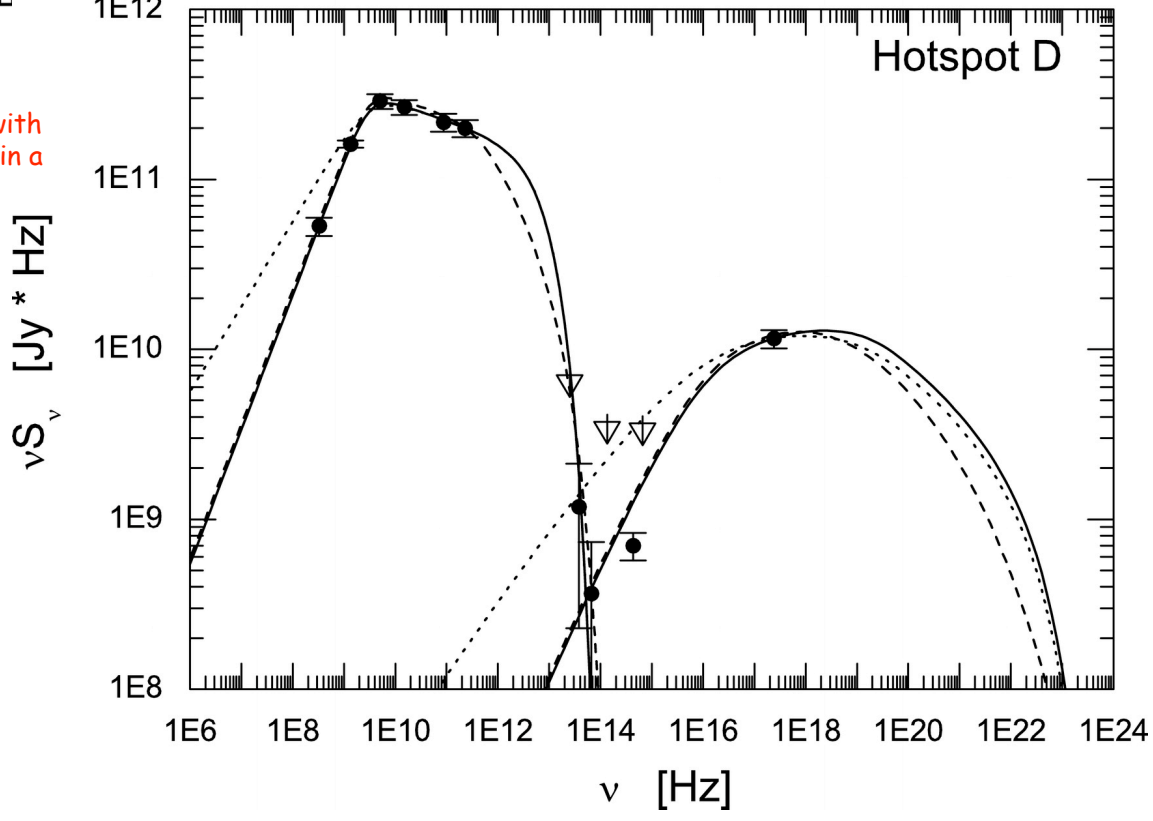

Shocks!

LS+ 07: for the low-energy electron index $s_1 \sim 1.5$, one has energy equipartition $U_p \sim U_e$ for the number density ratio $N_e/N_p \sim 10$, as claimed for the blazar sources.

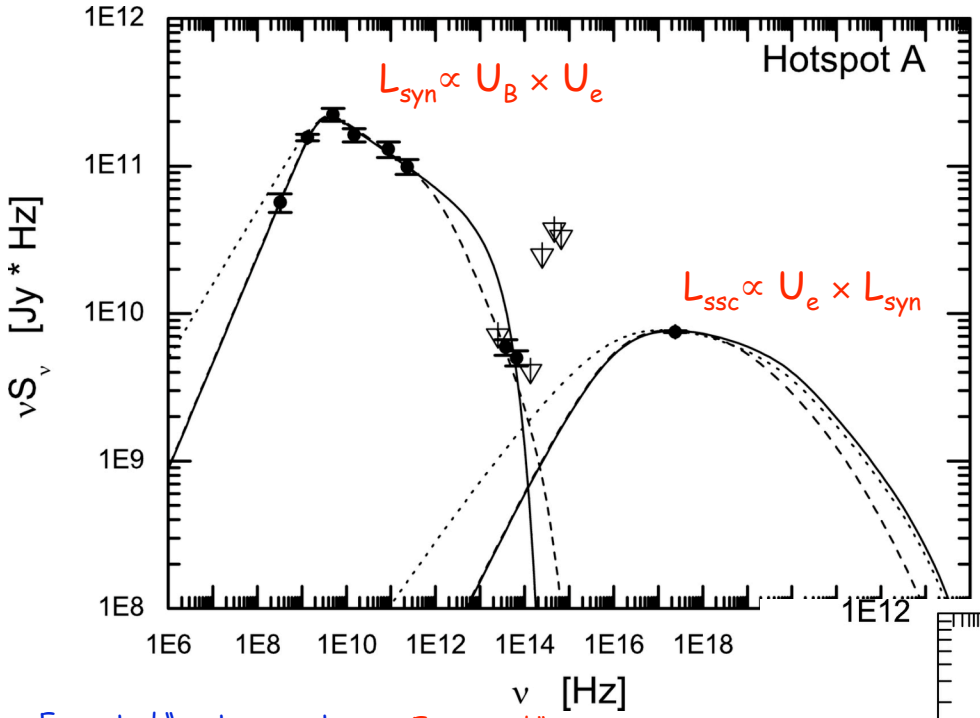

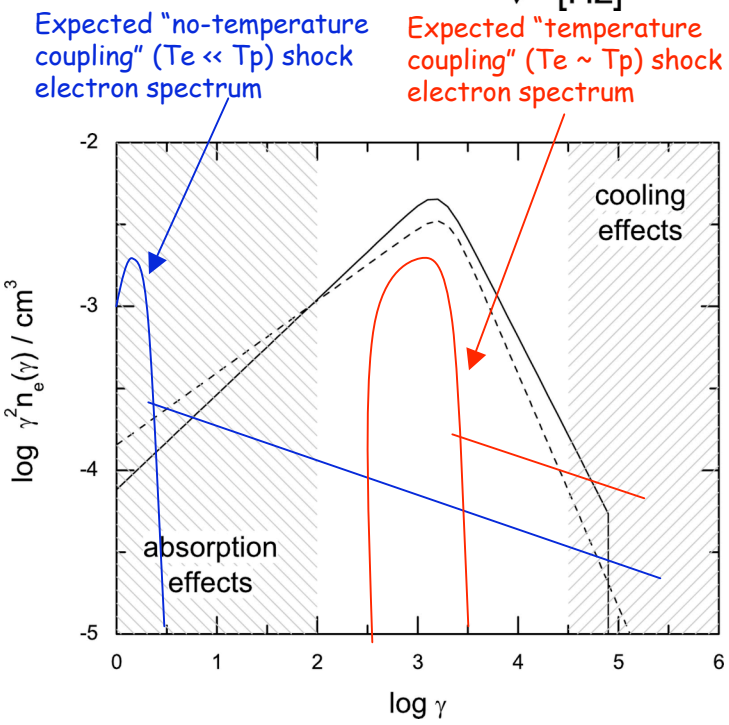

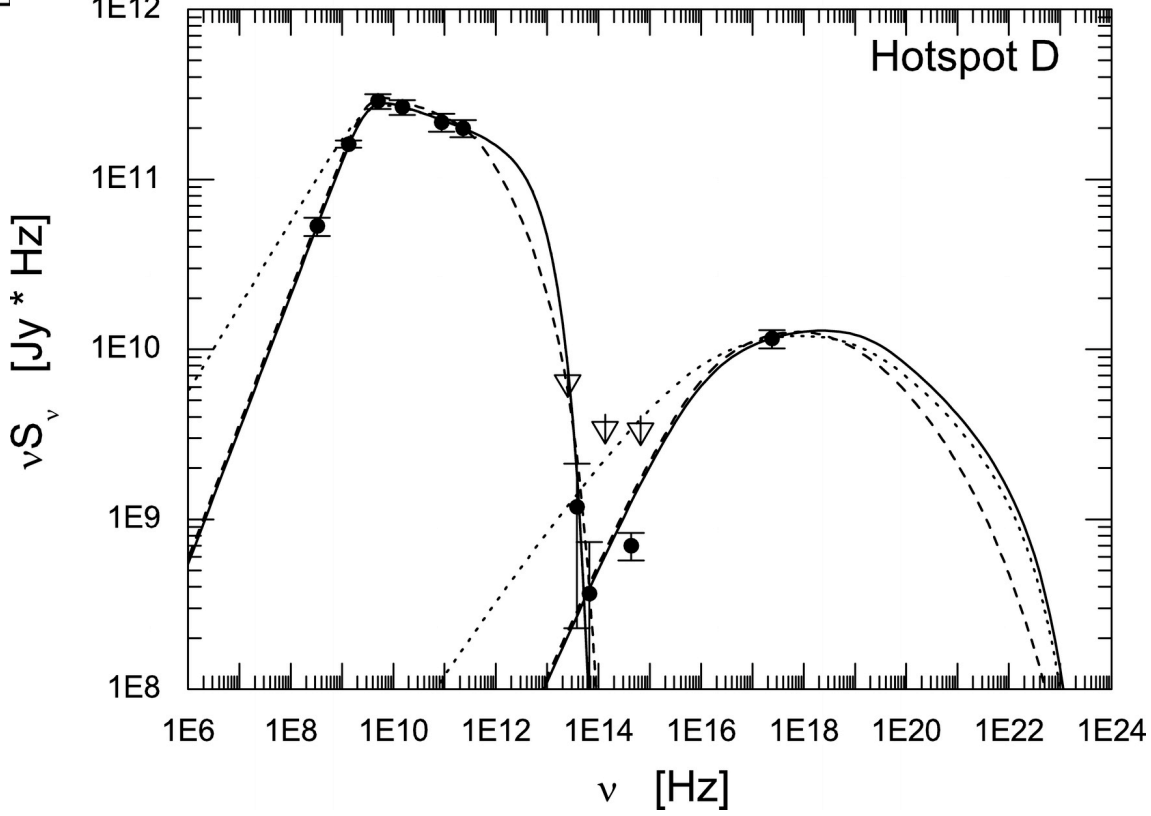

Lobes

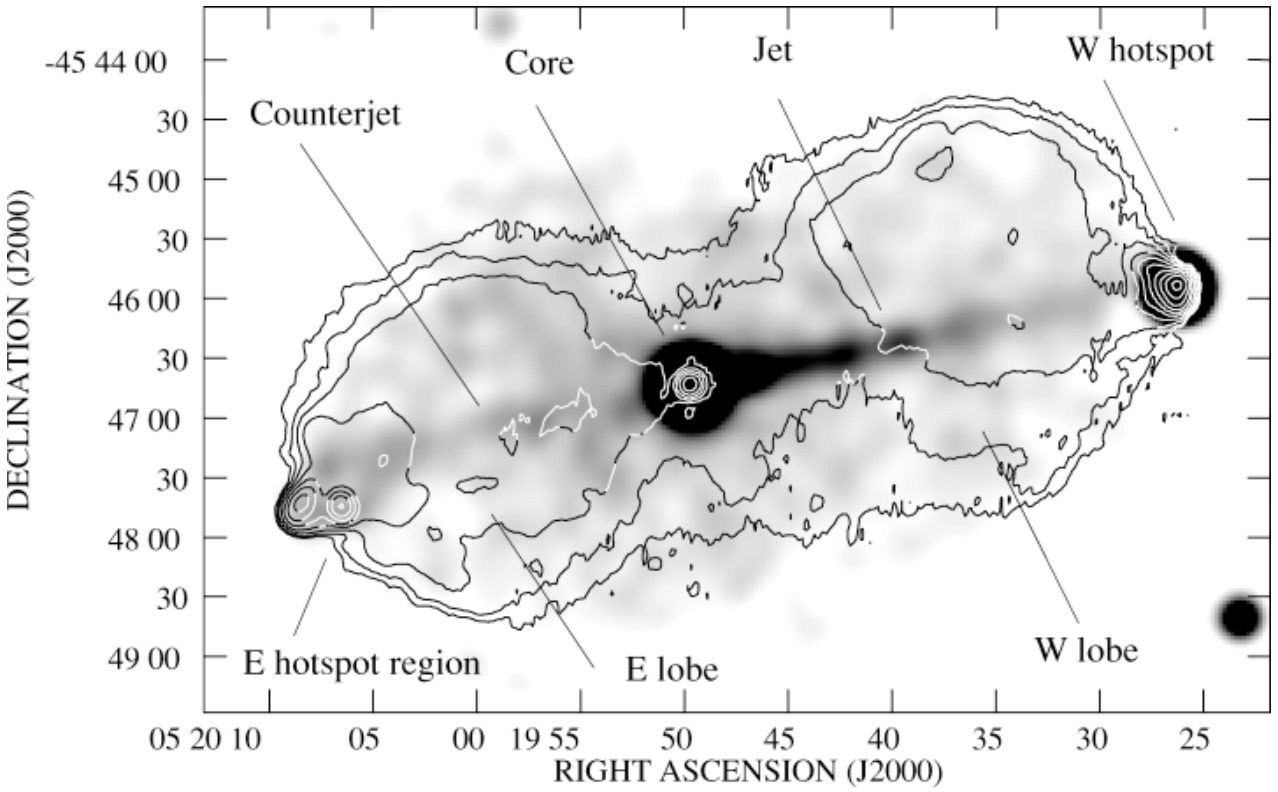

Expected inverse-Compton X-ray emission from radio lobes of powerful radio galaxies and quasars (**Harris & Grindlay 79**) was detected first in Fornax A (**Feigelson+ 95** and **Kaneda+ 95**), and later in many analogous systems (e.g., Pictor A; **Hardcastle & Croston 05**).

X-ray and radio lobe emission in this and many other analogous sources (**Croston+ 05, Kataoka & LS 05**) indicates rough energy/pressure equipartition

$U_B \sim U_e$

The IC emission is expected to extend up to GeV photon energy range at the level detectable by Fermi/LAT (**Cheung 07, Georganopoulos+ 08, Hardcastle+ 09**).

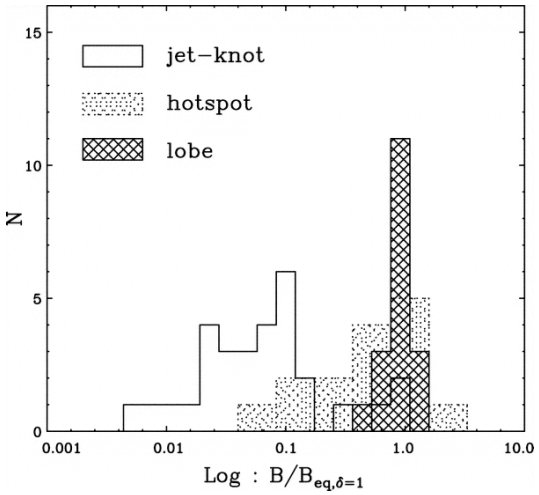

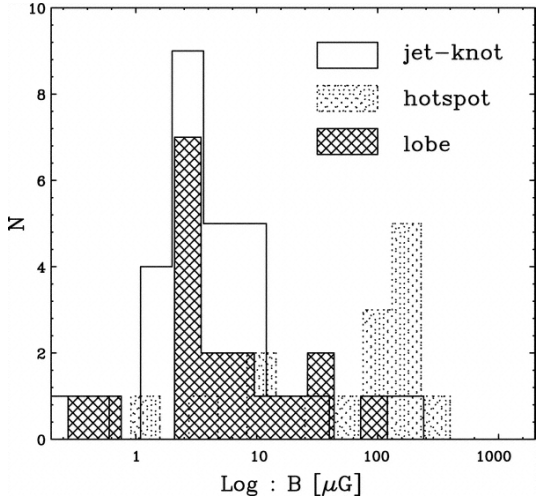

Bow Shocks

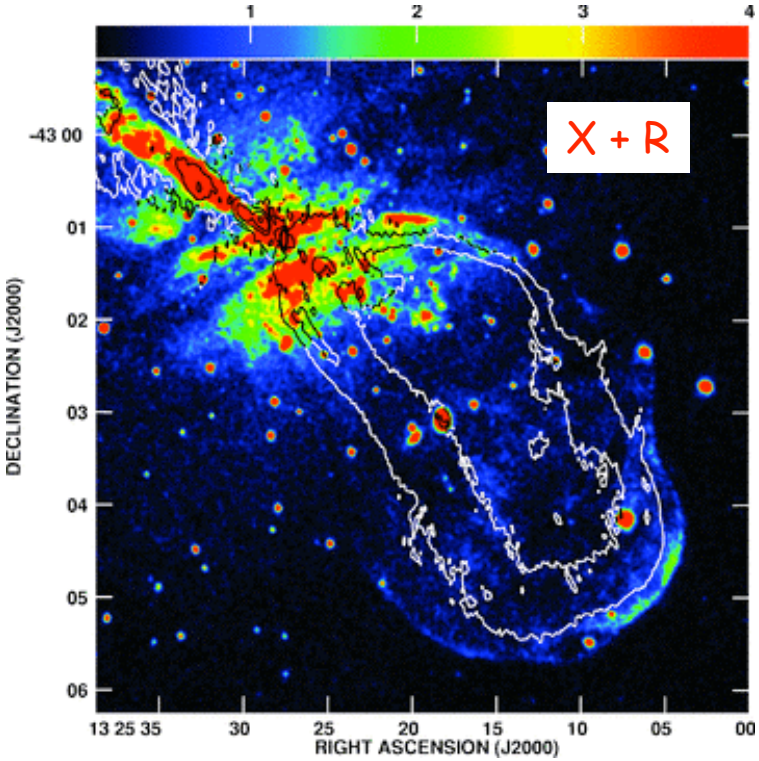

The inner counterlobe in Centaurus A radio galaxy: instead of the expected thermal X-ray emission (due to compressed IGM), the synchrotron X-ray emission observed, indicating the presence of 100 TeV energy electrons (B_{eq} ~ 10 μG, v_{sh} ~ 0.01 c, M_{sh} ~ 8) (**Croston+ 09**).

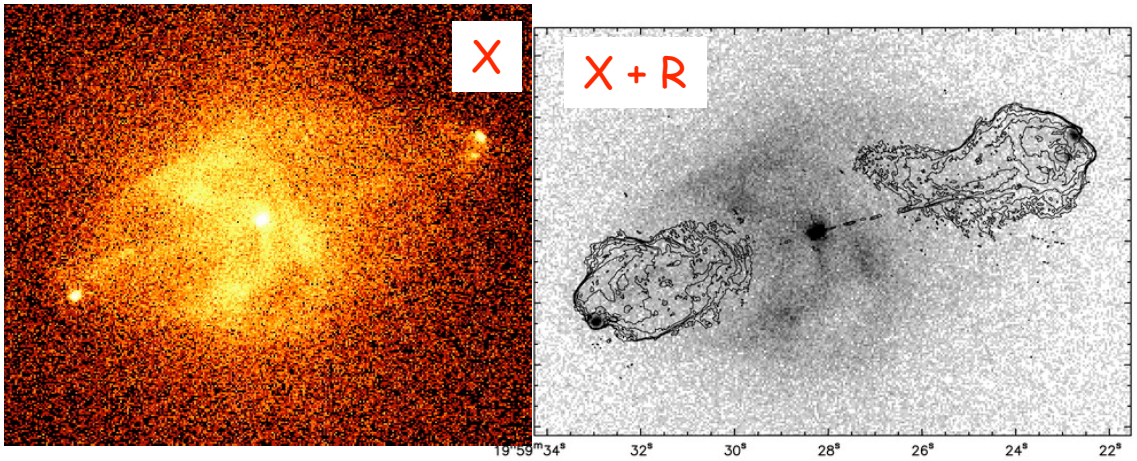

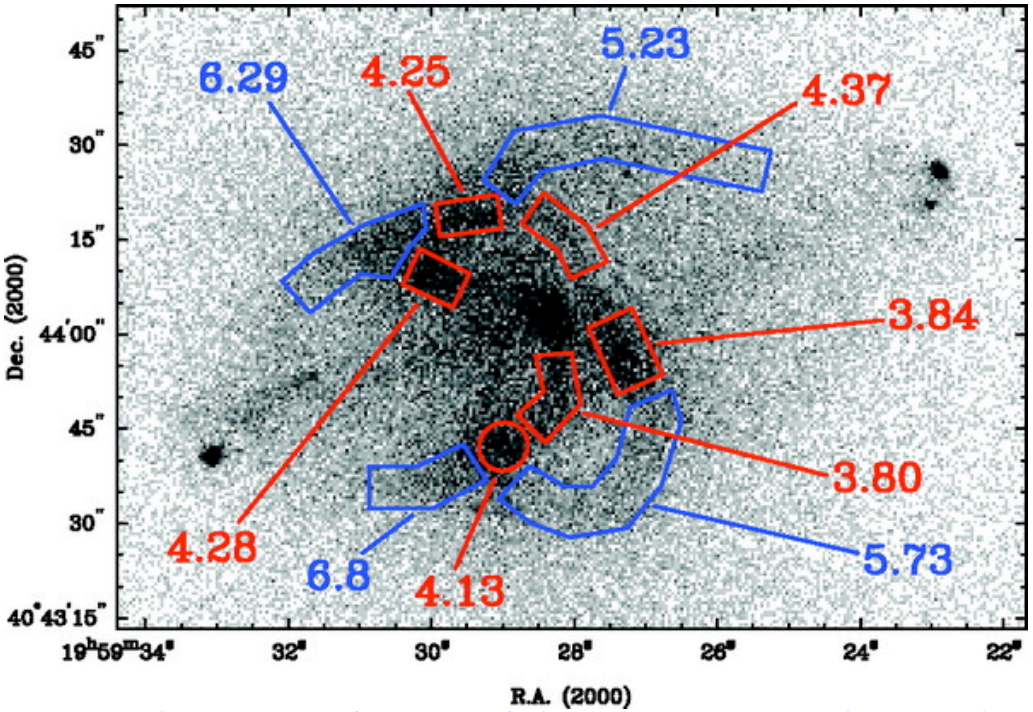

In the case of powerful radio sources located in clusters only very weak bow shocks (not easily!) detected with Chandra (e.g., Cygnus A radio galaxy: v_{sh} ~ 0.003 c, M_{sh} ~ 1.3; **Wilson+ 06, few other exampes - Nulsen+ 05a, 05b**).

Conclusions

- Broad-band non-thermal emission of extragalactic jets seems to be entirely leptonic in origin (SYN and IC). No radiative signatures of relativistic protons; however, several indications for the dynamical role of cold (non- or mildly-relativistic) protons.
- No indications for the magnetic field amplification. Instead, a need for an effective conversion of Poynting flux-dominated outflow to the matter dominated one at some distance from the central engine. Shock regions seem to be characterized by a rough pressure/energy equilibration between different plasma species (p+, e+-, B).
- Electron spectra hardly consistent with any universal power-law form. Instead, variety of electron spectra observed: broken power-laws (with indices $s_1 \sim 1\text{-}2$, $s_2 \sim 2\text{-}4$), curved spectra (ultrarelativistic Maxwellians?), etc. Maximum electron energies observed up to ~100 TeV.
- In addition to localized particle acceleration sites, distributed (turbulent) acceleration processes at work.